



저작자표시-비영리-변경금지 2.0 대한민국

이용자는 아래의 조건을 따르는 경우에 한하여 자유롭게

- 이 저작물을 복제, 배포, 전송, 전시, 공연 및 방송할 수 있습니다.

다음과 같은 조건을 따라야 합니다:



저작자표시. 귀하는 원저작자를 표시하여야 합니다.



비영리. 귀하는 이 저작물을 영리 목적으로 이용할 수 없습니다.



변경금지. 귀하는 이 저작물을 개작, 변형 또는 가공할 수 없습니다.

- 귀하는, 이 저작물의 재이용이나 배포의 경우, 이 저작물에 적용된 이용허락조건을 명확하게 나타내어야 합니다.
- 저작권자로부터 별도의 허가를 받으면 이러한 조건들은 적용되지 않습니다.

저작권법에 따른 이용자의 권리는 위의 내용에 의하여 영향을 받지 않습니다.

이것은 [이용허락규약\(Legal Code\)](#)을 이해하기 쉽게 요약한 것입니다.

[Disclaimer](#)

**Ph.D. DISSERTATION OF ENGINEERING**

**Direct, rapid antimicrobial susceptibility  
testing for expediting optimal antibiotic  
treatment of bloodstream infection**

혈류 감염에서 적정 항생제의 신속 처방을 위한  
초고속 항균제 감수성 검사

**FEBRUARY 2020**

**DEPARTMENT OF TRANSDISCIPLINARY STUDIES**

**GRADUATE SCHOOL**

**SEOUL NATIONAL UNIVERSITY**

**HYUN YONG JEONG**

## **Abstract**

# **Direct, rapid antimicrobial susceptibility testing for expediting optimal antibiotic treatment of bloodstream infection**

Sepsis is the systemic response to microbial infection including bloodstream infection over whole body. The risk of mortality increases by 9% with every hour that administration of the accurate antimicrobial treatment is delayed. Approximately 250,000 cases of sepsis occur in the United States annually. The mortality rates of sepsis patients are 20~30%, which is two~three times of those of stroke and cardiovascular diseases. For the treatment of septic patients, the rapid antimicrobial resistance profiling against various antimicrobials is necessary. It took 3 days from blood extraction to the termination of antimicrobial susceptibility for sepsis diagnosis in clinical settings. There are 1~10 CFU/mL of pathogens inside the blood from septic patients, which is quite low for further tests.

Thus, the bacterial enrichment such as is compulsory prior to the antimicrobial susceptibility testing (AST). After blood culture, the pure culture process is needed to isolate pure colonies from blood cultures. Then accurate antimicrobial can be identified after these experimental procedures. Our group has proposed bacterial immobilization and single cell morphological analysis for reduction of total turnaround time of sepsis diagnosis. Through these core technology, our group was able to reduce the turnaround time of AST from 12 hours to 3 hours.

From this dissertation, I proposed the direct, rapid antimicrobial susceptibility testing (DRAST) without subsequent pure culture process after blood culture. This DRAST system was able to produce highly accurate AST results within 6 hours. I utilized high-throughput 96 well format micropatterned biochip. This micropattern inside biochip enabled stable agarose matrix loading. Different from previous AST research from our group, another diffusion approach is utilized. This usage of another diffusion eliminated diffusion limits from previous results using lateral diffusion approach. There was a diffusion limit due to the lateral diffusion of

antimicrobials, leading to the ununiformity of bacterial patterns inside agarose matrix. Since DRAST system utilizes large-area time-lapse imaging, lateral diffusion approach was not appropriate.

In this dissertation, I tried to develop the DRAST system which could be applicable in real clinical settings. The lyophilization of antimicrobials was one of the efforts. With this lyophilization of antimicrobials, the preparation process of DRAST system was comparatively easier compared to previous AST reports. As the DRAST chip has an embedded focus mark at the bottom of biochip, the automated time-lapse imaging of same area was possible with subsequent automated image processing. With this image acquisition and analysis, it was able for me to confirm the antimicrobial susceptibility against various antimicrobials. With companion bacterial identification technology, matrix-assisted laser desorption ionization -time-of-flight mass spectrometer (MALDI-TOF MS), we were able to get antimicrobial susceptibility results from 300 clinical strains from clinical settings, satisfying the recommended AST guidelines of the Clinical &

Laboratory Standards Institute (CLSI).

In summary, the DRAST system, the direct, rapid antimicrobial susceptibility testing proposed from this dissertation was able to reduce the total turnaround time of sepsis diagnosis from 3 days to 30 hours. This DRAST system can tell the results of accurate antimicrobial prescriptions which are highly needed for septic patients. As this DRAST system is developed at the highly applicable level composed of high-throughput, micropatterned biochip and automated time-lapse acquisition/analysis, these technical features raise the applicability of this system in real clinical settings. With these advantages, the DRAST system can contribute to current sepsis diagnostics and to solve the global-wide antimicrobial resistance problem

**Keywords:** Sepsis, Rapid antimicrobial susceptibility test, Biochip, Single colony tracking, Antimicrobial resistance

**Student Number:** 2014-24882

# Table of Contents

<b>ABSTRACT .....</b>	<b>I</b>
<b>TABLE OF CONTENTS .....</b>	<b>V</b>
<b>LIST OF TABLES.....</b>	<b>IX</b>
<b>LIST OF FIGURES .....</b>	<b>XII</b>
<b>CHAPTER 1. INTRODUCTION .....</b>	<b>1</b>
<b>1.1. Background about sepsis .....</b>	<b>2</b>
1.1.1. What is sepsis? .....	2
1.1.2. Current sepsis diagnostics procedures .....	5
<b>1.2. Emerging sepsis diagnostics (AST) technology.....</b>	<b>6</b>
1.2.1. Need of rapid sepsis diagnostics (AST) technology .....	7
1.2.2. Emerging molecular sepsis diagnostics (AST) technology.....	8
1.2.3. Emerging phenotypic sepsis diagnostics (AST) technology .....	9
<b>1.3. Main concept of the dissertation and previous works of our group in</b>	

<b>rapid AST .....</b>	<b>1 1</b>
1.3.1. Previous work of rapid AST in our research group .....	1 1
1.3.2. Main Concept: Direct, rapid antimicrobial susceptibility testing (DRAST) from positive blood cultures .....	1 6
 <b>CHAPTER 2. PLATFORM DEVELOPMENT .....</b>	<b>2 0</b>
 <b>2.1. The concept and experimental steps of DRAST system .....</b>	<b>2 1</b>
2.1.1. The concept and experimental steps of DRAST system.....	2 1
2.1.2. Direct detection of antimicrobial resistance from positive blood culture bottles	2 2
2.1.3. DRAST validation with spike-in sample .....	2 8
2.1.4. Positive blood culture bottles .....	2 8
2.1.5. The number of bacteria in PBCBs.....	2 9
2.1.6. Image acquisition in DRAST .....	3 1
2.1.7. Colony formation monitoring.....	3 3
 <b>2.2. Design and fabrication of DRAST chip.....</b>	<b>3 3</b>

2.2.1.	Diffusion limit and gradient generation.....	3	3
2.2.2.	Application of lyophilization for DRAST chip.....	4	0
<b>2.3.</b>	<b>DRAST system as an inoculum effect free system .....</b>	<b>4</b>	<b>3</b>
2.3.1.	Inoculum effect .....	4	3
2.3.2.	The validation of DRAST system to be no inoculum effect .....	4	4
<b>2.4.</b>	<b>Automatic AST using microcolony-forming area detection using image processing algorithm.....</b>	<b>5</b>	<b>1</b>
<b>CHAPTER 3.</b>	<b>PLATFORM VALIDATION: DRAST SYSTEM WITH MALDI-TOF MS .....</b>	<b>6</b>	<b>0</b>
<b>3.1.</b>	<b>Direct identification of bacteria from positive blood culture bottles.</b>	<b>6</b>	<b>1</b>
3.1.1.	The workflow of direct identification of bacteria from positive blood culture bottles.....	6	1
3.1.2.	Our workflow of direct identification of bacteria from positive blood culture bottles.....	6	2
<b>3.2.</b>	<b>Clinical Study of DRAST with MALDI-TOF MS.....</b>	<b>6</b>	<b>3</b>
3.2.1.	The accuracy and discrepancy results of clinical study of DRAST with		

MALDI-TOF MS .....	6 3
3.2.2. The total turnaround results of clinical study of DRAST with MALDI-TOF MS	7 6
<b>3.3. Clinical Study of DRAST of Gram-positive clinical strains with MALDI-TOF MS .....</b>	<b>7 7</b>
3.3.1. The performance of DRAST system against Gram-positive cocci with MALDI-TOF MS .....	7 8
3.3.2. Discussions of performance of DRAST system against Gram-positive cocci with MALDI-TOF MS .....	8 2
<b>CHAPTER 4. CONCLUSION.....</b>	<b>8 3</b>
<b>BIBLIOGRAPHY.....</b>	<b>8 8</b>

# List of Tables

Table 1.1 Determination criteria of systemic inflammatory response syndrome [6] .....	3
Table 1.2 Translational status of sensing technologies for pathogen identification and monitoring host responses (Reprinted from [13]).....	7
Table 1.3 Selected examples of emerging molecular methods for rapid antimicrobial susceptibility testing (AST) (Reprinted from [16]).....	9
Table 1.4 Selected examples of emerging phenotypic methods for rapid antimicrobial susceptibility testing (AST) (Reprinted from [16]).....	10
Table 1.5 Summary of previous research in rapid AST from our group .....	16
Table 2.1 MIC values from DRAST with spiked sample, broth microdilution test and CLSI quality control ranges. The DRAST test was performed on a positive blood culture sample spiked with four standard strains. The broth microdilution test was performed on a colony cultured on an LB agar plate. Each test was performed in three times. (Reprinted from [11]).....	27
Table 2.2 The heating process during the freeze-drying process. After freezing tray, freezing trap and vacuum process in freeze-drying, the tray was heated for decrease the water content in antibiotics. The heating process was composed of several sequences .....	41
Table 2.3 Number of bacteria in the well and field of view (FOV). We diluted the PBCBs by 1/100. On average, the final concentration was $9.4 \times 10^6$ CFU/ml. After mixing with agarose at a 1:3 volume ratio, the concentration was $2.3 \times$ $10^6$ CFU/ml. In this case, the final concentration in the well was $2 \times 10^4$ CFU, and there were approximately 100 bacteria cells in the field of view of the 20X lens with a 5x tube lens. (Reprinted from [11]).....	46
Table 2.4 Summary of a comparison of AST results from various inoculum sizes of <i>E. coli</i> ATCC 25922, <i>P. aeruginosa</i> ATCC 27853, <i>S. aureus</i> ATCC 29213	

and *E. faecalis* ATCC 29212. “Correct” means a case with identical MIC values from different inoculum sizes. “One two-fold” and “Two two-fold” denote cases with MIC values from different inoculum sizes that were different by two-fold and four-fold, respectively. “Essential agreement” refers to the proportion of cases that were correct or had one two-fold difference. The essential agreement rates were 99.33% in *E. coli* ATCC 25922, 100% in *P. aeruginosa* ATCC 27853, 95.37% in *S. aureus* ATCC 29213 and 100% in *E. faecalis* ATCC 29212. (Reprinted from [11]) ..... 5 0

Table 2.5 Optimized threshold values. The general threshold value to determine the MIC was 0.2. The threshold values were optimized in the following cases. (Reprinted from [11]).....	5 6
Table 2.6 MIC values from DRAST with spiked sample, broth microdilution test and CLSI quality control ranges. The DRAST test was performed on a positive blood culture sample spiked with four standard strains. The broth microdilution test was performed on a colony cultured on an LB agar plate. (Reprinted from [11]).....	5 9
Table 3.1 Bacterial ID of 206 clinically isolated strains. There were 16 species of 105 Gram-negative strains and 7 species of 101 Gram-positive strains. (Reprinted from [11]).....	6 4
Table 3.2 Classification of clinical samples for MIC interpretive standards. (Reprinted from [11]).....	6 5
Table 3.3 Discrepancy rates and CA rates for DRAST using clinical samples. The DRAST results were compared with the BMD results to calculate the discrepancy rates. For the BMD test: S, susceptible; I, intermediate; R, resistant. For DRAST: mE, minor error; ME, major error; VME, very major error; CA, categorical agreement.....	6 6
Table 3.4 Summary of clinical testing of Gram-negative strains using DRAST, according to the antimicrobial applied. (Reprinted from [11]) .....	6 7
Table 3.5 Summary of clinical testing of Enterobacteriaceae spp. strains using DRAST, according to the applied the antimicrobial applied. (Reprinted from	

[11]).....	6 8
Table 3.6 Summary of clinical testing of <i>Pseudomonas aeruginosa</i> strains using DRAST, according to the antimicrobial applied. (Reprinted from [11])..	6 9
Table 3.7 Summary of clinical testing of <i>Acinetobacter</i> spp. strains using DRAST, according to the antimicrobial applied. (Reprinted from [11]).....	7 0
Table 3.8 Summary of clinical testing of Gram-positive strains using DRAST, according to the antimicrobial applied. (Reprinted from [11]).....	7 0
Table 3.9 Summary of clinical testing of <i>Staphylococcus</i> spp. strains using DRAST according to the applied antimicrobial applied.....	7 1
Table 3.10 Summary of clinical testing of <i>Enterococcus</i> spp. strains using DRAST according to the antimicrobial applied.....	7 2
Table 3.11 Distribution of Gram-positive cocci from PBCs used in this study (Reprinted from [25]).....	7 8
Table 3.12 Agreement rates in AST results between DRAST system and MicroScan WalkAway plus system for Gram-positive cocci (Reprinted from [25]).....	7 9
Table 3.13 Discrepancy rates and agreement rates of two AST systems in this clinical evaluation classified into combination of antimicrobial agents and bacterial species (Reprinted from [25]).....	8 1

# List of Figures

Figure 1.1 The stages of sepsis .....	3
Figure 1.2 Current sepsis diagnosis procedures.....	5
Figure 1.3 The schematic diagram and antimicrobial susceptibility testing process for microfluidic agarose channel (MAC) system. This MAC chip was fabricated with PDMS and PDMS-coated glass [33] ....	1 2
Figure 1.4 Minimal inhibitory concentration (MIC) determination through time-lapse imaging and image processing. (A) The MIC determination of <i>S.aureus</i> ATCC 29213 against gentamicin. (B) The MIC determination of <i>P.aeruginosa</i> ATCC 27853 against gentamicin. The scale bars represent 50 $\mu\text{m}$ .....	1 3
Figure 1.5 The schematic figures of rapid AST platform which utilizes single cell morphological analysis inside microfluidic agarose channels. (A) Comparison of rapid AST via single cell tracking and conventional AST based on turbidimetry (B) The schematic of MAC chip integrated with 96-well platform for high-throughput analysis (C) Experimental procedures of the MAC chip .....	1 4
Figure 1.6 Morphological categorization of single cells against antibiotics. After time-lapse imaging of the single bacterial cells, their growth patterns against the antibiotics were analyzed and classified into four groups [24] .....	1 5
Figure 1.7 The main concept of DRAST system: Direct AST system processing wide dynamic range of inoculum sizes from positive blood cultures [11, 25].....	1 6
Figure 2.1 (A) The conventional AST system requires three separate culture processes: blood culture for positive infection detection, subculture for separation of bacteria from blood cells, and AST via	

optical density measurement; the total time to result is approximately 60 hours. The direct and rapid AST (DRAST) system developed herein does not require a subculture process and enables AST to be performed in six hours. The total time to result of DRAST is less than 24 hours. (B) Process of preparing a DRAST chip from a PBCB. A PBCB aliquot was diluted and mixed with liquid-state agarose. The mixture was inoculated into a DRAST chip consisting of 96 test wells containing various antimicrobials at different concentrations. (C) Detailed structure of a DRAST chip well. Each test well consists of a micropatterned radial chamber for agarose matrix molding and a satellite well for freeze-dried antimicrobials. Inset images show the micropatterned chamber i) before agarose mixture loading and ii) after agarose mixture loading. (D) Experimental process for detecting bacteria in blood. A sample from a PBCB is mixed with agarose and loaded into the loading chamber in the chip. Freeze-dried antibiotics are rehydrated by adding culture media. Automated microscopic imaging is used to detect the growth of pathogens. Inset scanning electron microscope (SEM) images show i) freeze-dried antibiotics in the satellite well and ii) the focus mark on the bottom of the chip for automated imaging. (E) In the initial state, pathogens were not detectable using a 20x magnification lens; only blood cells were detectable. After four hours of incubation, in the case of resistance to the antibiotic, a single bacterium divided and formed a microcolony. Filled triangle represents a blood cell. Unfilled triangle represents a bacterial micro-colony. The scale bar represents 10 mm in (B), 3 mm in (C), 300  $\mu\text{m}$  in (D), and 100  $\mu\text{m}$  in (E). (Reprinted from [11]) 2 4

Figure 2.2 Time-lapse images of colonies from different dilution factors. (a) The raw sample from the PBCB was mixed with agarose. (b) A 10x dilution sample from PBCB. (c) A 100x dilution sample from PBCB. The scale bar represents 100  $\mu\text{m}$ . (Reprinted from [11]).. 2 6

Figure 2.3 Number of bacterial pathogens in PBCBs. The average number of pathogens was about $9.4 \times 10^8$ CFU/ml. The highest concentration was about $2.5 \times 10^9$ CFU/ml, and the lowest was about $5.6 \times 10^7$ CFU/ml. (Reprinted from [11]).....	3 1
Figure 2.4 The schematic figures of loading antimicrobials into agarose matrix in previous MAC chip (Reprinted from [24]).....	3 3
Figure 2.5 Images of bacteria inside the agarose matrix in different regions without antibiotics after 6 hours of incubation. The growth difference can be easily detected. (Reprinted from [24]).....	3 4
Figure 2.6 (A) The six different imaging regions. (B) Time-lapse images of <i>E. coli</i> treated with gentamicin at two different concentrations at the different locations. In regions 1–4, near the antibiotic well, the responses of the bacteria were identical. In regions 5 and 6, the bacteria divided regardless of antibiotic concentration. Scale bar, 25 $\mu$ m. (C) The number of bacteria according to the each region in (B). (Reprinted from [24]).....	3 5
Figure 2.7 The comparative schematic figures of the diffusion approach between previous MAC chip and DRAST chip [11, 24].....	3 6
Figure 2.8 The schematic design of initial prototype for DRAST chip....	3 7
Figure 2.9 Time-lapse images in DRAST prototype (Figure 2.8) PMMA chip.....	3 8
Figure 2.10 The design candidates of DRAST chip for stable loading agarose matrix.....	3 8
Figure 2.11 Images of top and perspective view and prototype of various designs.....	3 9
Figure 2.12 The perspective view of DRAST chip consists of 4 main chambers with connected the satellite well .....	4 0
Figure 2.13 The results of food dye solution after freeze-dry process.	4 2
Figure 2.14 The illustrated figure of the example of inoculum effect..	4 3

- Figure 2.15 Colony formation of bacteria at different inoculum sizes. In all inoculum sizes from  $5.0 \times 10^7$  to  $5.0 \times 10^5$  CFU/ml, there was microcolony formation at 0, 0.25 and 0.5  $\mu\text{g/ml}$  gentamicin. At 1  $\mu\text{g/ml}$  gentamicin, there was no colony formation at any inoculum size. The scale bar represents 100  $\mu\text{m}$ . (Reprinted from [11])..... 4 5
- Figure 2.16 MIC values from different *E. coli* ATCC 25922 inoculum sizes of  $5.0 \times 10^7$ ,  $5.0 \times 10^6$  and  $5.0 \times 10^5$  CFU/ml incubated with 17 clinically important antimicrobials and analyzed using DRAST and broth microdilution test. For all inoculum sizes, the MIC values were in the middle of the CLSI quality control ranges. (Reprinted from [11])..... 4 8
- Figure 2.17 Consistent AST results from a wide range of inoculum sizes. MIC values from different *E. coli* ATCC 25922 inoculum sizes of  $5.0 \times 10^7$ ,  $5.0 \times 10^6$  and  $5.0 \times 10^5$  CFU/ml incubated with tobramycin and analyzed using DRAST and broth microdilution test. (Reprinted from [11])..... 4 9
- Figure 2.18 (A) Time-lapse images were acquired from the automated imaging system, and the image data were transferred to the analysis system. (B) Time-lapse images of *K. pneumoniae* with several concentrations of amoxicillin/clavulanic acid (A/C). (C) The raw images from (B) were processed to binary format images. The number of white pixels in the image represents the microcolony area. The scale bars in (B) represent 100  $\mu\text{m}$ . (Reprinted from [11]).... 5 2
- Figure 2.19 Image processing for microcolony detection. (a) The raw image acquired from the imaging system. (b) The result of sharpening and binarization. (c) The detected contours of the microcolonies recognized in (b). The scale bar represents 300  $\mu\text{m}$  (Reprinted from [11])..... 5 3
- Figure 2.20 (A) Graph of the microcolony-forming area in Figure 2.19C. From low A/C concentrations until 16/8  $\mu\text{g/ml}$ , there was a

substantial increase in microcolony-forming area in the images. However, from 16/8 µg/ml to 32/16 µg/ml, there was no substantial change in the area of bacteria. **(B)** The normalized growth rates at all the concentrations were calculated. Values higher than 20% were regarded as growth, and lower values were regarded as non-growth. From low A/C concentrations until 16/8 µg/ml, the normalized growth rates were higher than 20% and regarded as growth. However, at 32/16 µg/ml, the normalized growth rate was 2.3% and lower than 20%; thus, it was regarded as non-growth. Therefore, the MIC value was determined to be 32/16 µg/ml. **(C)** Final AST report. Using the ID information and MIC interpretive criteria from CLSI, antibiotic susceptibility was determined in a full antimicrobial panel..... 5 4

Figure 2.21 Time-lapse detection of decelerated growth rate due to antimicrobial effect (A) Time-lapse detection of S.aureus to the antibiotic erythromycin. (B) Time-lapse detection of E.faecalis to the antibiotic erythromycin. (Reprinted from [11]) ..... 5 8

Figure 3.1 Procedures between studies to perform identification directly from positive blood cultures (Reprinted from [44])..... 6 2

Figure 3.2 Number of bacteria in clinical PBCB samples. (a) Gram-negative strain bottle. The highest concentration was approximately  $7.6 \times 10^9$  CFU/ml, and the lowest was approximately  $1.3 \times 10^8$  CFU/ml. (b) Gram-positive strain bottle. The highest concentration was approximately  $7.6 \times 10^9$  CFU/ml, and the lowest was approximately  $1.6 \times 10^7$  CFU/ml. (Reprinted from [11])..... 6 5

Figure 3.3 Time-lapse images of microcolonies of Staphylococcus hominis with trimethoprim/sulfamethoxazole. In the raw images, few microcolonies were visible. However, some of the microcolonies were out of focus and not detected in the processed images. The scale bar represents 300 µm. .... 7 3

Figure 3.4 CA rates according to the main classified strains:

*Enterobacteriaceae* spp. (n=87, 89.9%), *P. aeruginosa* (n=9, 88.9%),  
*Staphylococcus* spp. (n=66, 92.1%), *Enterococcus* spp. (n=35, 95.4%).  
 Error bars represent 95% confidence intervals. (Reprinted from [11])  
 ..... 7 4

Figure 3.5 Discrepancy rates according to the main classified strains:  
*Enterobacteriaceae* spp. (mE=7.9%, ME=2.6%, VME=1.2%), *P.*  
*aeruginosa* (mE=11.1%, ME=0.0%, VME=0.0%), *Staphylococcus*  
 spp. (mE=4.7%, ME=3.8%, VME=2.4%), and *Enterococcus* spp.  
 (mE=4.3%, ME=0.0%, VME=0.6%). The error rates were calculated  
 by comparing the AST results from each method with the BMD test.  
 Error bars represent 95% confidence intervals. (Reprinted from [11])  
 ..... 7 5

Figure 3.6 Average time to results of AST from (A) time of positive  
 detection of blood culture bottles or (B) time of blood collection from  
 patient. The time required for AST using DRAST and a conventional  
 AST method requiring subculture (Vitek 2 or MicroScan) was  
 calculated. (Reprinted from [11])..... 7 6

# Chapter 1.

## Introduction

In this chapter, a short background about sepsis and current sepsis diagnostics will be introduced. After introduction of background knowledge about sepsis, state-of-art trends in sepsis diagnostics such as microbial culture and susceptibility testing technologies and the clinical value of these emerging sepsis diagnostic technology will be described. After that, previous technical innovations of our group in rapid antimicrobial susceptibility testing will be introduced. Finally, the subject of this dissertation, direct, rapid antimicrobial susceptibility test from positive blood cultures based on microscopic imaging analysis for expedite sepsis diagnosis will be presented. This technology eliminates the need for subsequent pure culture process after blood culture, which has been one of the major bottleneck for reducing the total turnaround time for sepsis diagnosis.

## **1.1. Background about sepsis**

### **1.1.1. What is sepsis?**

Sepsis is the life-threatening dysfunction of organs due to a dysregulated immune system which is fighting an infection. This disease is associated with the existence of pathogenic microorganisms or their derived toxins in the bloodstream [1]. Globally, almost 30 million people are suffering from this lethal disease. Of these, two-thirds experience severe sepsis and one-sixth die [2]. From various data, it is suggested that an incidence of 3 million cases of sepsis worldwide per year in neonates and 1.2 million cases per year in children, with mortality rates ranging from 11~19% [3]. In the United States hospitals, sepsis is not only the most expensive condition to treat but also the leading cause of mortality with reports estimating as many as 3.1 million cases at a cost of \$24 billion per year and mortality rates ranging between 20% and 50%.[4]

The infection is normally caused by pathogens which manage to escape attacks from the immune system and they begin to spread throughout the whole body, eventually causing widespread release of cytokines that begins the organ dysregulation [5]. As a result, sepsis progresses through several stages as shown in Figure 1.1. SIRS is the presence of two or more of the following criteria, typically denoted by relatively high or low body temperature, high heart rate, high respiratory rate and high or low white blood cell counts. These signs are used to identify systemic inflammatory response syndrome (SIRS). Sepsis is defined as

SIRS in response to an infectious process. The specific diagnosis criteria to determine whether it is SIRS or not is described in the Table 1.1.

Findings	Value
Temperature	$<36^{\circ}\text{C}$ or $>38^{\circ}\text{C}$
Heart rate	$>90/\text{min}$
Respiratory rate	$>24/\text{min}$
WBC	$<4 \times 10^9/\text{L}$ , $>12 \times 10^9/\text{L}$

Table 1.1 Determination criteria of systemic inflammatory response syndrome [6]

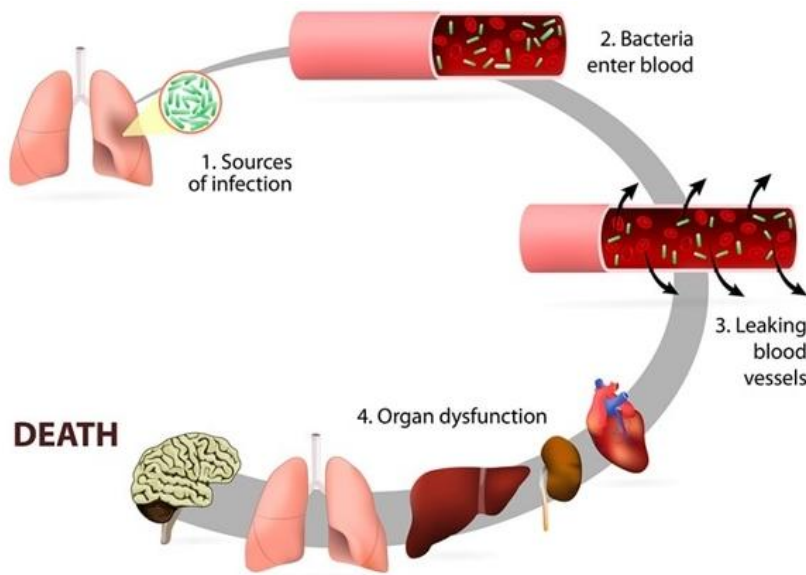


Figure 1.1 The stages of sepsis

The first stage is SIRS, characterized by abnormal temperature, heart rate, respiratory rate and the number of white blood cells, all caused by large scale

dysregulation of inflammatory cytokines. Besides pathogens inside the bloodstream, fragments of pathogens such as peptidoglycan, lipoteichoic acid, lipopolysaccharide (LPS) and endotoxins can also induce a strong immune response. If patients who is suspected to be sepsis, remain untreated, may have high possibility of the progress to severe sepsis, the SIRS is the presence of two or more of the following criteria, typically denoted by relatively high or low body temperature, high heart rate, high respiratory rate and high or low white blood cell counts. The second stage is severe sepsis, a symptom that acute organ dysfunction starts. A severe sepsis can also diagnosed when hypotension (low blood pressure) or hypoperfusion (decreased blood flow through an organ) occurs inside patients. Septic shock is the most severe stage of sepsis, as defined as the existence of hypotension induced by sepsis. This severe state has the highest chance of the mortality, estimates ranging from 30% to 50% [7].

Sepsis, this systemic response to infection including bloodstream infection, afflicts approximately 18 million people worldwide each year, and the risk of mortality rises by 9% with every hour that the appropriate antibiotic treatment is delayed. Due to the emergence and intensification of antimicrobial resistance, the prescription of empirical, broad-spectrum antibiotics is controlled by hospital antibiotic stewardship programs [8]. Thus, fast and accurate confirmation of antimicrobial susceptibility of pathogens is necessary to improve the clinical prognosis in patients with sepsis and antibiotic resistant bacterial infection [9].

### 1.1.2. Current sepsis diagnostics procedures

The total turnaround time (TAT) of current sepsis diagnostic is longer than three days since it necessitates three overnight culture steps: blood culture, subculture and antimicrobial susceptibility test (AST) culture.

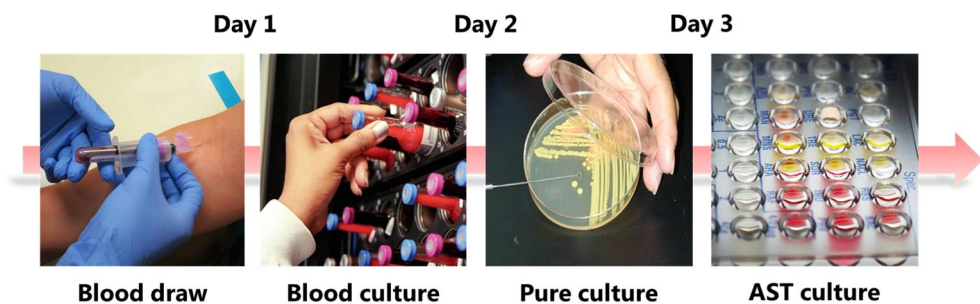


Figure 1.2 Current sepsis diagnosis procedures

Blood culture, the current state-of-the-art method, is a microbiological culture of blood extracted from patients, it checks for foreign biological substances such as bacteria, yeast and other microorganisms in blood. Thus, it's highly important test for blood infections because they can be led to another serious complications such as sepsis. It provides necessary identification of responsible organisms for sepsis, appropriate choice of empirical or selected antibiotics and selections required to find out the source of infection [10]. The following descriptions are several stages of blood culture.

- 1) Blood extraction from patients, collected aseptically into blood culture bottle
- 2) Blood culture bottle placed in the blood culture bottle incubator

- 3) Monitoring the pathogen growth until the positivity is confirmed
- 4) In case of positivity appears in the blood culture machine, the cultured pathogen is subcultured on different types of agar plates to obtain purified form of colonies.

As the pathogen concentration inside the patient's blood ranges from 1cfu/mL to 100cfu/mL, which highly insufficient for subsequent susceptibility testing, there needs cultivation period of 16~24 hours. Normally, blood culture takes 1 day to confirm the positivity from blood culture bottles in clinical settings. The pathogen concentrations from positive blood culture bottles span  $10^7\sim 10^9$  cfu/mL depending on the sample [11]. The pure culture process that subcultured pathogens are being overnight grown on the agar plate in the incubator, is conducted. Then, this purified form of pathogen colonies are utilized for the susceptibility testing. As most of current utilized susceptibility testing machines are based on the turbidity measurement, this pure culture process is inevitable. This whole blood culture diagnostic procedures are time-consuming and labor-intensive, typically taking 3 days to obtain the susceptibility results of patients. However, as once previously introduced, this lethal disease, sepsis can progress in a matter of hours [12].

## **1.2. Emerging sepsis diagnostics (AST) technology**

To combat this lethal disease and correlated antimicrobial resistance, which has been a global healthcare threat, the development of rapid sepsis diagnostics has been ongoing. As currently existing pathogen detection methods are unable to

detect and identify pathogens of low concentrations in biological samples, it is of high significance to develop alternative technology which is able to detect in ultrasensitive manner. Nowadays, there have been some efforts to tackle current technical bottlenecks using state-of-art technologies. The following table is the brief description of translational status of sensing technologies for pathogen identification and for monitoring host responses [13].

Technology or biomarkers	Tech/Biomarker is FDA approved	Current method	Blood volume (mL)	Time to result	Translational status	Commercial status	Commercial entities
Bacterial growth	Yes	Blood culture	15~20	1~5 Days	Clinical	Prototype	BacterioScan ImpeDx
Pathogen identification	Yes	DNA ampli. PCR	<0.05	1~2 hours	Clinical	Commercial	T2 Biosystems Qvella FAST Bruker MALDI Roche Septifast Biofire Filmarray
Antibiotic susceptibility test	Yes	Agar/Broth dilution assay	<0.05	1 day	Clinical	Prototype	Accelerate Pheno Q-Linea
Enumeration of blood cells	Yes	Haematology analyzer	<5	30 minutes	Clinical	Clinical	CytoBuoy NanoCollect Beckman Coulter (DXH900)
Circulating proteins (PCT, CRP)	Yes	Immuno analyzers	<10	30 minutes	Clinical	Clinical	Biomerieux (VIDAS) Elecsys BRAHMIS Abbott I-STAT
Small molecules	Yes	Blood gas analyzers	<10	<15 minutes	Clinical	Clinical	Abcam L-lactate Abbott I-STAT Roche COBAS

Table 1.2 Translational status of sensing technologies for pathogen identification and monitoring host reponses (Reprinted from [13])

### 1.2.1. Need of rapid sepsis diagnostics (AST) technology

In the face of uprising threats from multi-drug resistant pathogens, there have been growing need for translational technologies. As introduced once before in the introduction, little progress had been made in past decades of development of diagnostics and therapeutics for sepsis. The primary reason for slow progress arises from the huge heterogeneity in the response of septic patients. This heterogeneity makes difficult the development of effective diagnostics and the prediction of

which cases will progress to lethal organ dysfunction. The current diagnostic strategy in clinical settings is focused on the antibiotic prescription, fluid resuscitation and vasopressors. Previously, a number of studies have proven that early profiling of sepsis cases with subsequent rapid treatment lead to the recovery of patients [14]. The following tables (Table 1.3 and Table 1.4) in section 1.2.2 and section 1.2.3 are the summary of selected examples of emerging molecular and phenotypic methods for rapid antimicrobial susceptibility testing (AST), which can act as primary sepsis diagnostics, leading to rapid treatment of targeted antimicrobials. Each of examples are classified based on the principle of core technology with pros and cons additionally.

### **1.2.2. Emerging molecular sepsis diagnostics (AST) technology**

On the other hand, molecular methods detects the antimicrobial susceptibility of pathogens based on molecular markers which confers resistance. Due to their technical characteristics, it takes relatively shorter periods to get the results. As they induce the lysis of pathogen prior to the assays, they can detect nonculturable pathogens. However, they often require sample processing steps to purify and amplify the target molecules. The current limit of detection of PCR-based methods span  $10^3\sim 10^4$  cfu/mL depending on the preprocessing [15]. Sometimes, the presence of resistance markers may not correlate with phenotypic resistance. The other bottleneck of these molecular methods are the fact that they may be more costly compared to conventional culture methods.

Technology	PCR tests	Electrochemical sensors
Technology principle	Amplification-based nucleic acid detection using PCR	Nucleic acid analysis using electrochemical detection
Example technologies	Biofire Filmarray, Cepheid Xpert, Seegene MagicPlex, Roche SeptiFast, BD GeneOhm MRSA	GeneFluidics electrochemical biosensor, Nanostructure microelectrodes
Pros	- Short turnaround time (hours) - Some PCR assays can be highly multiplexable	- Less prone to the matrix effects of physiological samples
Cons	- Typically detect a limited set of preidentified genes and therefore cannot detect many of the ESBLs and CREs - Not able to cover rapid and complex evolving mechanisms - Culture-independent PCR may not work well for complex specimens such as blood - Limited and variable clinical sensitivity	- Limited LOD in blood samples
Technology	Microarray and nano/microparticle systems	Mass spectroscopy
Technology principle	Nucleic acid analysis mediated by hybridization on solid supports, including microarrays or particle	Analysis of species-specific molecular signatures
Example technologies	Nanosphere Verigene Luminex Xtag T2 Biosystems T2MR	Bruker MALDI Biotyper BioMerieux VITEK MS IRIDICA BAC BSI assay
Pros	- Highly multiplexable - Can be very sensitive	- Can cover a very broad range of species
Cons	- A preculture or nucleic acid purification and amplification step may still be required	- Relatively bulky and expensive
Technology	Sequencing technologies	Host responses
Technology principle	Genetic targets of bacteria are determined using WGS, NGS, or miniaturized sequencing technologies	Detection based on host gene expression on pathogen infection and immune responses
Example technologies	Oxford Nanopore technologies DNA Electronics LiDia	Immuneexpress Gene panel for sepsis
Pros	- Can analyze the extensive genetic polymorphism of resistant bacteria - Miniaturized sequencing technologies can analyze DNA sequence in real time and in an interactive manner, and therefore shorten assay time	- Assays can be developed based on publicly available gene expression and sequencing data
Cons	- Most of the current sequencing methods involve complex workflow, still slow turnaround time, and relatively high cost	- Still lacking assay platforms rapid enough to detect host responses

Table 1.3 Selected examples of emerging molecular methods for rapid antimicrobial susceptibility testing (AST) (Reprinted from [16])

### 1.2.3. Emerging phenotypic sepsis diagnostics (AST) technology

Phenotypic methods monitors bacterial growth or growth inhibition, metabolism and viability in the presence of the antimicrobial drugs. These methods are highly sensitive for cultivable pathogens and rather definitive in antibiotic susceptibility profiling. However, as they rely on the bacterial growth, they are

typically slow and inefficient to detect unculturable or relatively slow growth organisms.

Technology	Microfluidic-based culture methods	Imaging technologies	Cellular mass and density
Technology principle	Monitoring bacterial growth in partitioned small volumes	Direct imaging of bacterial growth, morphology, motion and other related phenotypes with antibiotic treatment	Measuring cellular mass and density, particularly at a single-cell level
Example technologies	Plugs, droplets, microwells	Microfluidic single-cell SCMA Digital microscopy of Accelerate Dx oCelloScope system BacterioScan laser scattering	Suspended microchannel resonator Microchannel cantilevers Affinity Biosensors
Pros	<ul style="list-style-type: none"> <li>- Confining single bacteria in small volumes reduces the time required to detect the bacteria</li> <li>- Antibiotic concentration gradient generation allows effective determination of MIC against antibiotics</li> <li>- Amenable for point-of-care (POC)</li> </ul>	<ul style="list-style-type: none"> <li>- Shorter turnaround time</li> <li>- Amenable for direct growth monitoring</li> <li>- Able to achieve single-cell sensitivity</li> </ul>	<ul style="list-style-type: none"> <li>- Single-cell sensitivity</li> </ul>
Cons	<ul style="list-style-type: none"> <li>- Input sample volume may be limited</li> <li>- Preenrichment of bacteria may be required</li> </ul>	<ul style="list-style-type: none"> <li>- Initial culture steps are often required</li> <li>- Complex algorithms are required for accurate bacterial phenotype analysis</li> </ul>	<ul style="list-style-type: none"> <li>- Often require preenrichment of bacteria and sample processing steps to obtain single cells prior to measurement</li> <li>- Low throughput</li> </ul>

Table 1.4 Selected examples of emerging phenotypic methods for rapid antimicrobial susceptibility testing (AST) (Reprinted from [16])

To reduce the total turnaround time (TAT) of current antibiotic resistance detection process, a variety of approaches had been proposed [11, 17-25]. Researchers have developed methods to observe division of pathogens at early incubation stage. Recently, a number of researchers have reported to reduce the time to results (TTR) of antimicrobial susceptibility testing. However, compared to rapid AST which reduces 10-12 hours, removing pure culture (subculture) process can further save additional 1 days of incubation. Disk diffusion method, also known as Kirby-Bauer method from blood culture inoculum was introduced as direct AST due to the fact that researchers at that time directly applied the pathogen sample. Many researchers did numerous trials to remove subculture process by

separating bacteria from positive blood culture bottles (PBCBs) using centrifugal separation method and erythrocyte lysis filtration method. The main purpose of these methods is to confirm the accurate concentration of pathogen for conventional turbidimetry-based AST. However, these separation processes prior to AST are highly time-consuming and necessitate multiple cumbersome preparation works which are not suitable to be used in clinical settings. For rapid AST without subculture process to be utilized in clinical settings, a new AST system handling a wide range of inoculum sizes of bacteria is necessary.

### **1.3. Main concept of the dissertation and previous works of our group in rapid AST**

#### **1.3.1. Previous work of rapid AST in our research group**

Our group has proposed and developed various high-throughput screening methods based on microparticles and biochips [26-32]. From these, our group reported the single cell tracking method for rapid antimicrobial susceptibility test of common pathogens including *E.coli*, *P. aeruginosa* and *S. aureus* [24, 33]. A microfluidic agarose channel (MAC) system was developed, reducing the AST assay time for determination of minimum inhibitory concentration (MIC) by single bacterial time-lapse imaging. Time-lapse images of single bacterial cells under different antibiotics and concentrations were acquired, then processed for MIC determination. The time to results of this rapid AST assay was obtained within 3~4

hours.

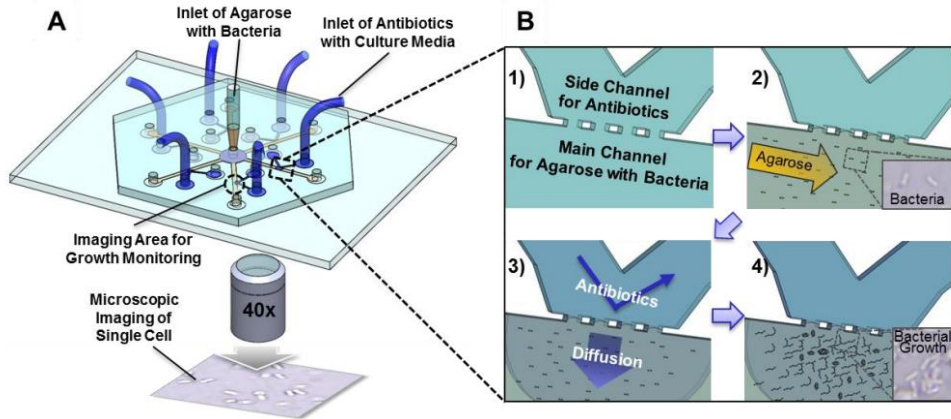


Figure 1.3 The schematic diagram and antimicrobial susceptibility testing process for microfluidic agarose channel (MAC) system. This MAC chip was fabricated with PDMS and PDMS-coated glass [33]

The agarose-bacteria mixture was injected into the center of the chip, flowing simultaneously into the six main channels with different concentrations of antimicrobials supplied from side-branched channels. Each interface between agarose matrix and antimicrobial solutions was monitored by 40x microscopic lens. (Figure 1.3) For the validation of this MAC system, three standard CLSI pathogens were tested to determine the MICs of 4 antimicrobials. MIC values of each antimicrobial was derived after 3 hours of time-lapse imaging and image processing. (Figure 1.4)

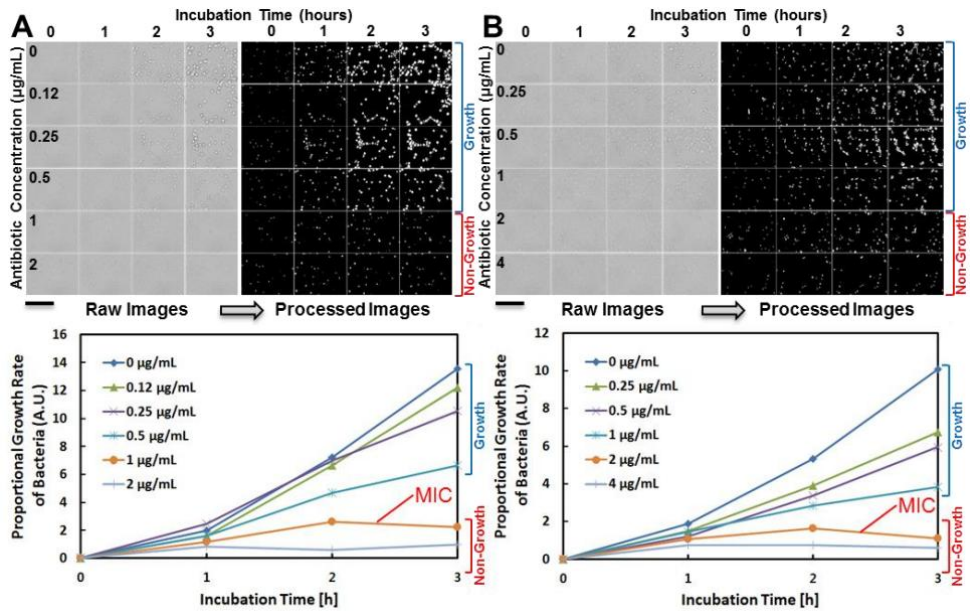


Figure 1.4 Minimal inhibitory concentration (MIC) determination through time-lapse imaging and image processing. (A) The MIC determination of *S.aureus* ATCC 29213 against gentamicin. (B) The MIC determination of *P.aeruginosa* ATCC 27853 against gentamicin. The scale bars represent 50 µm

To fulfill the accuracy requirements of AST, our group proposed and demonstrated a single-cell morphological analysis by observation of morphological changes of bacterial cells under different antimicrobials (Figure 1.5) [24]. Instead of applying same image processing algorithm, our group applied adaptive image processing algorithms considering both changes in cell mass and morphological changes. (Figure 1.6) After screening numerous experimental results, bacterial cell morphologies were classified into four subtypes composed of division, no change, filamentary formation, and swelling.

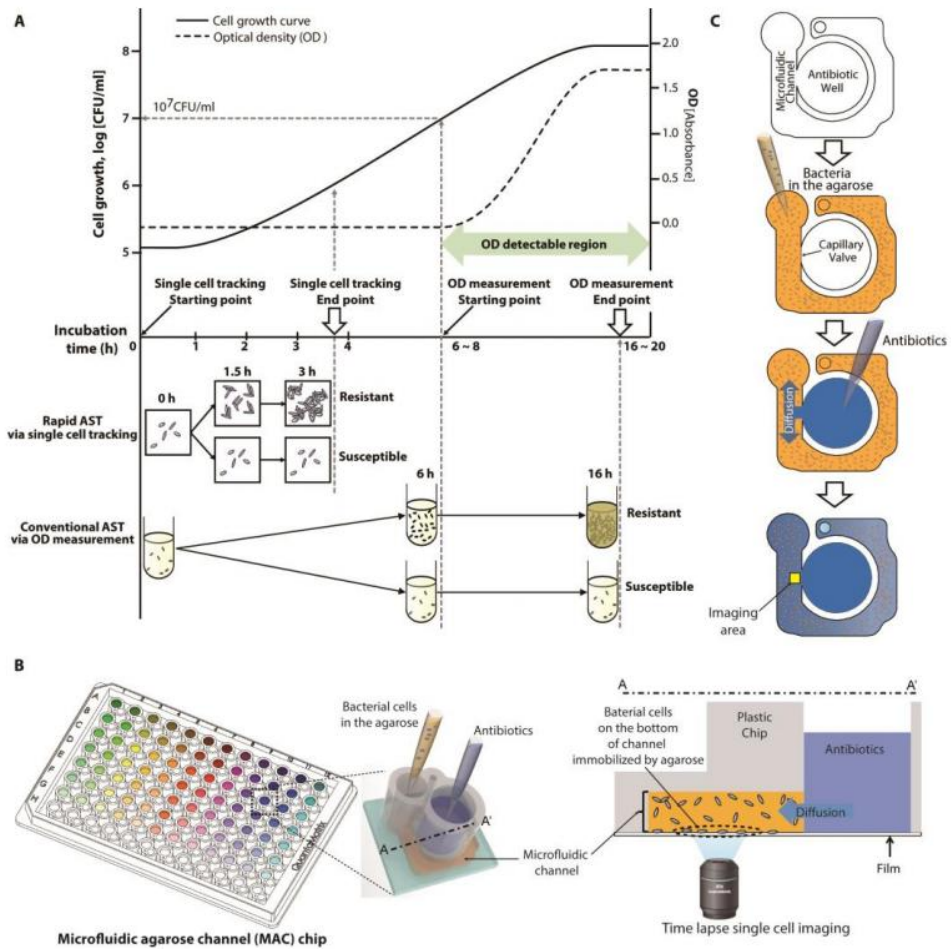


Figure 1.5 The schematic figures of rapid AST platform which utilizes single cell morphological analysis inside microfluidic agarose channels. (A) Comparison of rapid AST via single cell tracking and conventional AST based on turbidimetry (B) The schematic of MAC chip integrated with 96-well platform for high-throughput analysis (C) Experimental procedures of the MAC chip

	Time lapse images			Morphological pattern	Numerical interpretation of morphology	Susceptibility determination	Cases
	0 h	1.5 h (*2 h)	3 h (*4 h)				
<b>A*</b> <i>S. aureus</i> with penicillin				Dividing		Resistant (under MIC)	General antimicrobials against all four standard strains
<b>B*</b> <i>E. faecalis</i> with vancomycin				No change		Susceptible MIC or over MIC	General antimicrobials against <i>S. aureus</i> and <i>E. faecalis</i> and Non $\beta$ -lactams against <i>P. aeruginosa</i> and <i>E. coli</i>
<b>C</b> <i>P. aeruginosa</i> with aztreonam				Filamentary formation			Penem class drug in $\beta$ -lactams against <i>P. aeruginosa</i> and <i>E. coli</i>
<b>D</b> <i>E. coli</i> with imipenem				Swelling formation		Resistant (under MIC)	$\beta$ -lactams drug except penem class against <i>P. aeruginosa</i> and <i>E. coli</i>
<b>E</b> <i>P. aeruginosa</i> with piperacillin				Filamentary formation and dividing			Penem class drug in $\beta$ -lactams against <i>P. aeruginosa</i> and <i>E. coli</i>
<b>F</b> <i>P. aeruginosa</i> with imipenem				Swelling formation and dividing			

Figure 1.6 Morphological categorization of single cells against antibiotics. After time-lapse imaging of the single bacterial cells, their growth patterns against the antibiotics were analyzed and classified into four groups [24]

This application of single cell morphological analysis (SCMA) method reduced discrepancy rates when compare to previous bacterial area measurement method for both beta-lactam and non-beta-lactam antimicrobials against Gram-negative bacterial strains. With previously proposed MAC channels and SCMA method, our group validated these works can be applied for rapid antimicrobial susceptibility testing in faster and more accurate manners. The summary of our group's previous works is as follows. (Table 1.5)

	<i>Lab chip (2013)</i>	<i>Science Translational Medicine (2014)</i>
<b>Technology</b>	Microfluidic agarose channel (MAC) Time-lapse imaging (40x microscopic imaging)	
<b>Test sample</b>	Pure culture samples	
<b>TAT of Tests</b>	3 ~ 4 hours (51 hours from blood extraction)	
<b>Analysis</b>	Bacterial area measurement (BAM)	Single cell morphological analysis (SCMA)
<b>Throughput</b>	6 wells per one chip	96 wells per one chip
<b>Materials</b>	PDMS	PC / PMMA
<b>Chip fabrication</b>	Soft-lithography	Injection molding
<b>Claims</b>	1) Usage of bacterial immobilization 2) Demonstration of image-based AST	1) Single cell morphological analysis 2) High-throughput AST enabled

Table 1.5 Summary of previous research in rapid AST from our group

### 1.3.2. Main Concept: Direct, rapid antimicrobial susceptibility testing (DRAST) from positive blood cultures

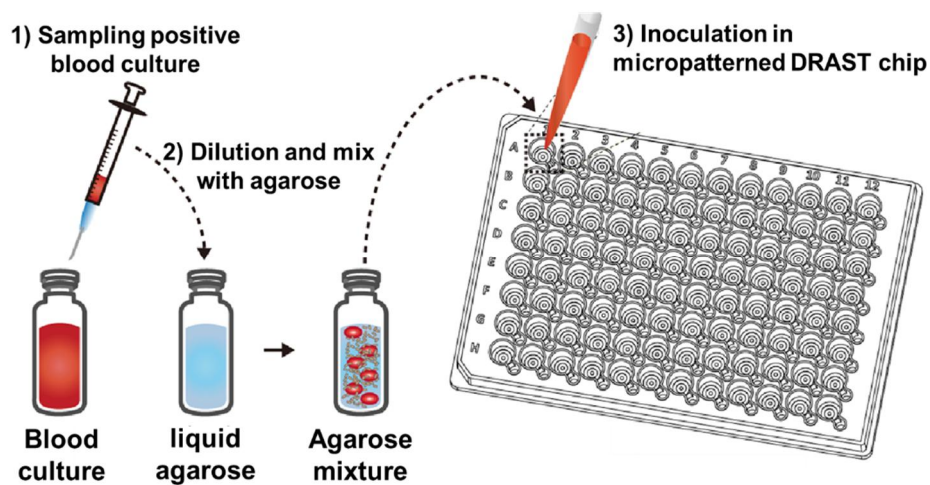
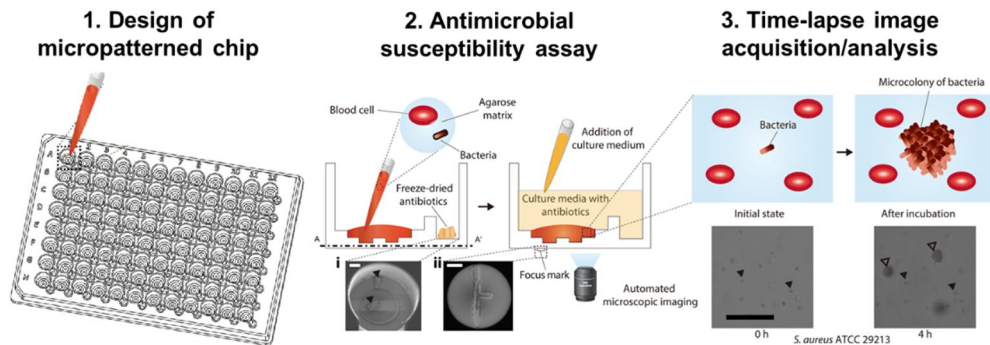


Figure 1.7 The main concept of DRAST system: Direct AST system processing wide dynamic range of inoculum sizes from positive blood cultures [11, 25]

The main theme of this dissertation is the development of a direct AST system that can handle a wide dynamic range of pathogen concentrations from PBCBs without prior separation process [11]. By direct sample processing PBCBs without measuring pathogen concentration, the demonstration of AST within less than 30 hours without sacrificing accuracy was achieved. The detection of antibiotic resistance of pathogens using relatively low microscopic imaging and micropattern-embedded polystyrene biochips was demonstrated instead of measuring the optical density (OD). For the interpretation of AST results from DRAST, the pathogen identification is essential. Therefore, DRAST was simultaneously performed with the direct ID system, MALDI Biotyper and Sepsityper kit from Bruker (Billerica, MA, United States). By satisfying the recommended performance criteria of the United States (U.S.) Food and Drug Administration (FDA), this study demonstrated the feasibility of using the DRAST system in clinical settings as a rapid AST for positive blood culture specimens. The direct use of PBCBs in this rapid AST system reduced the turnaround time to appropriate antimicrobial treatment by two days compared to conventional systems.

For the timely treatment of patients with infections in bloodstream and cerebrospinal fluid, a rapid antimicrobial susceptibility test (AST) is of high significance. The list of limitations of previous researches and the proposed solutions in this dissertation to resolve them are as follows.



- (1) Direct, rapid antimicrobial assay needs to be developed. Most of current rapid AST methods utilizes pure culture samples after 2 days of consecutive culture composed of blood culture and pure culture due to their technical limitations from turbidimetry dependence. This prolongs the total turnaround time to prescribe accurate antimicrobials for patients. I developed a direct, rapid AST method which can handle positive blood culture bottles right after blood culture of 1 day incubation.
- (2) For handling wide range of bacterial concentrations inside positive blood culture bottles, the platform needs optimized chip design for this purpose. Previous microfluidic agarose channel (MAC) chip developed from our group, utilized lateral diffusion of antimicrobials from satellite wells, showing diffusion gradients. This diffusion gradient can make discrepancies during the interpretation of time-lapse acquired images. Thus, I applied another diffusion approach in terms of antimicrobials with modified design of micropatterned chip to eliminate diffusion gradient and limit within same well.

- (3) As there need a number of antimicrobials for profiling antimicrobial susceptibility testing, high-throughput form of system is necessary. In addition, the preparation of various kinds and concentrations of antimicrobials are required, I applied lyophilization method in the antimicrobial preparation process with suitable chip design for this.
- (4) To develop user-friendly system in clinical settings, the system should be designed with the consideration of automation. Thus, I embedded imprinted focus mark at the bottom of each well in DRAST chip for automated focus mark detection and image acquisition. As our group previously successfully demonstrated automated image processing with time-lapse acquired images, we integrated this hardware and software for further user compatibility. As a result, DRAST system was demonstrated as a full automated system, from image acquisition to image analysis

The outline of this dissertation is as follows. In chapter 2, the developmental process of the platform will be described by dividing it into five subsections as shown above. In chapter 3, the validation of the proposed platform for the direct, rapid AST will be demonstrated. In chapter 4, a pathogen capture technology for rapid microbial culture will be discussed. In final chapter 5, I will discuss the meaning of the proposed platform and the potential impact of my work.

# Chapter 2.

## Platform Development

In this chapter, the entire developmental process of DRAST system is divided into five parts. (1) The concept and experimental steps of DRAST system. This section will describe the concept of DRAST system, the direct detection of antibiotic resistance from positive blood cultures is possible. The detailed experimental procedures of DRAST system from positive blood culture to image analysis and data interpretation will be discussed. (2) The design and fabrication of DRAST chip. In this section, the fabrication and criteria which I considered in the design of chip will be discussed. (3) The consistency of DRAST system handling wide range of inoculum sizes. In this section, the consistent results of DRAST system regardless of the concentration of bacteria will be demonstrated. (4) The performance of DRAST system as an automatic AST system through the microcolony-forming area detection using image processing algorithm. In this section, the image processing algorithm and the optimization of threshold values will be described.

## **2.1. The concept and experimental steps of DRAST system**

### **2.1.1. The concept and experimental steps of DRAST system**

After a positive signal from the BACTEC FX (Becton Dickinson Company, NJ, United States) or BacT/ALERT® (bioMerieux Inc., Marcy l'Étoile, France) 3D automated blood culture machine, a sample for DRAST system was collected from the BACTEC or BacT/ALERT® blood culture bottle with a syringe. After Gram stain, polymicrobial and yeast samples were excluded as they cannot be handled. Components in the blood culture bottles such as antimicrobials and bacteriostatic factors or antimicrobial absorption materials could affect the AST results. To get the optimum inoculation concentration and to eliminate the effects of substances in the bottles, a 10 µl sample was collected from the bottle and diluted 100-fold with 990 µl of culture media. (Figure 2.2) Then, 300 µl of the diluted sample was mixed with 900 µl of liquid-state immobilization agent, 0.5% agarose at 37–40 °C in 1:3 volume ratio. Next, 10 µl of the mixture of agarose and was inoculated in the radial-shaped chamber of a 96-well format DRAST chip. (Figure 2.1B) Due to the capillary effect, the micro-patterned radial shape of the well helped the mixture of PBCB and agarose spread and form a disk matrix in the entire well. (Figure 2.1C) This radial shape micro-patterns of the well eliminated occasional diffusion limit with the stabilization of agarose mixture to the bottom side of the chip. After solidification of the agarose mixture at room temperature, 100 µl of culture medium was loaded into the satellite well to rehydrate the freeze-dried antibiotics.

(Figure 2.1D) The culture medium with antimicrobials was diffused into the agarose of bacteria matrix. The imaging plane in the z-axis was 150  $\mu\text{m}$  from the interface between the agarose matrix and antimicrobials. The thickness of the agarose matrix was 300  $\mu\text{m}$  and antimicrobials were dispersed evenly over all regions of the agarose matrix. The whole preparation of the 96-well DRAST chip was done within less than five minutes. After the preparation, DRAST chip was incubated in a 37  $^{\circ}\text{C}$  chamber. A focus mark was imprinted at the bottom of the chip for automatic tracking of the image region in the chip. (Figure 2.1D) Using the focus mark, the same location in the agarose matrix was imaged every two hour using a time-lapse method. The field of view of the image was 1126.4 x 594  $\mu\text{m}$ . At the beginning, only erythrocytes were mostly observable in the image. After a few hours of incubation, the bacteria in the agarose matrix formed a three-dimensional colony, which was detected after four hours. (Figure 2.1E) It is considered that the micro-colony formed due to the resistant characteristic of the bacteria to a certain antimicrobial. Cases with no micro-colony formation were considered indicative that the bacterial strain was susceptible to antimicrobials.

### **2.1.2. Direct detection of antimicrobial resistance from positive blood culture bottles**

The positive blood culture bottle sample contained an average concentration of  $10^9$  CFU/ml of bacterial cells mixed with blood cells, and the

microcolonies were too small for their formation to be detected. (Figure 2.2) To validate the performance of the DRAST system, direct AST was performed using spiked samples of four standard Clinical and Laboratory Standards Institute (CLSI) strains – *E. coli* ATCC 25922, *S. aureus* ATCC 29213, *P. aeruginosa* ATCC 27853, and *E. faecalis* ATCC 29212 – in blood culture bottles. When the PBCB sample was mixed with agarose, only red blood cells and white blood cells of size 7-15  $\mu\text{m}$  were initially detectable. After incubation, bacterial cells in the agarose matrix had divided, and had formed the micro-sized colony larger than 20  $\mu\text{m}$ , which was detectable. (Figure 2.1E) Using this scheme, it possible for us to determine antibiotic resistance directly from PBCBs. The minimum inhibitory concentration (MIC) was derived using micro-sized colony detection from images acquired in time-lapse manner and was compared with the MIC value from the BMD test, the golden standard AST method (Table 2.1). The MIC values from RAST were consistent with the values from BMD and were within the CLSI quality control (QC) ranges. This supports that the results from DRAST chip using colony detection are coincident with standard test. Thus, results from DRAST are feasible to determine the AST results of bacteria with antibiotics. Therefore, the detection of bacterial microcolonies in an agarose matrix was validated as a direct and rapid AST method for PBCB samples.

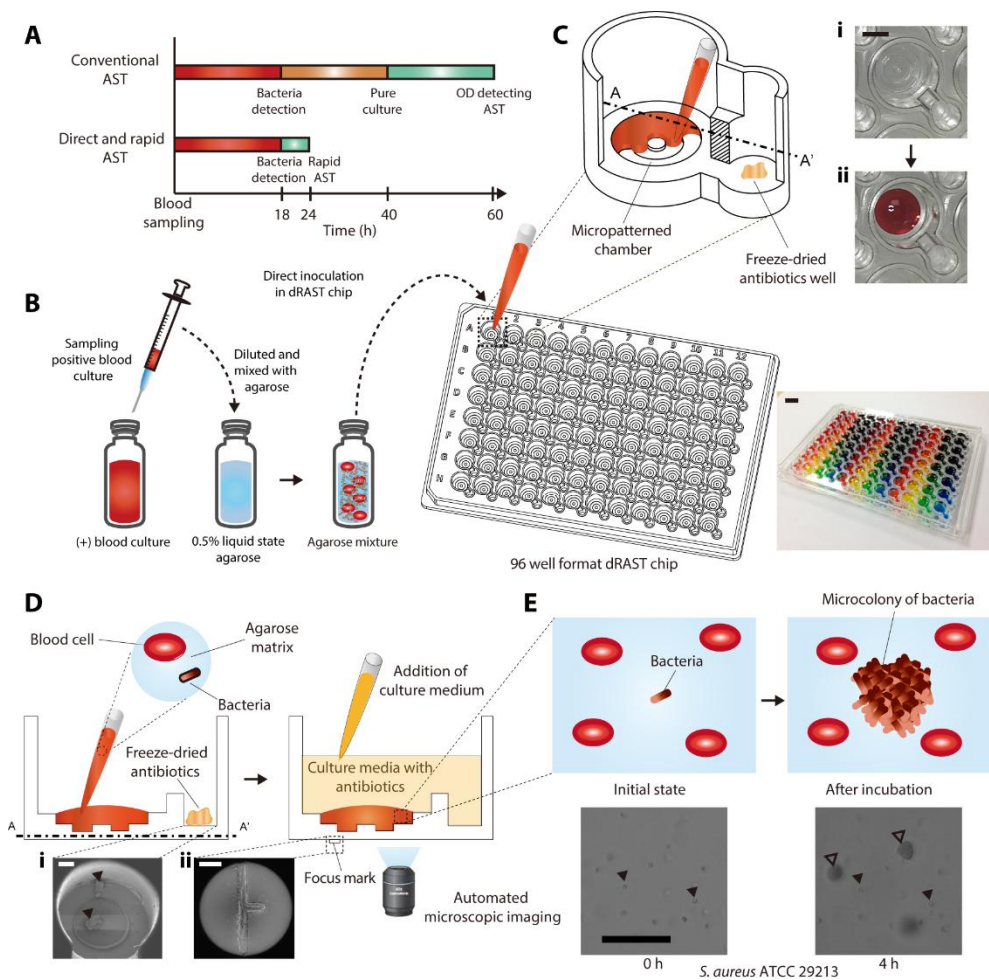


Figure 2.1 (A) The conventional AST system requires three separate culture processes: blood culture for positive infection detection, subculture for separation of bacteria from blood cells, and AST via optical density measurement; the total time to result is approximately 60 hours. The direct and rapid AST (DRAST) system developed herein does not require a subculture process and enables AST to be performed in six hours. The total time to result of DRAST is less than 24 hours. (B) Process of preparing a DRAST chip from a PBCB. A PBCB aliquot was diluted

and mixed with liquid-state agarose. The mixture was inoculated into a DRAST chip consisting of 96 test wells containing various antimicrobials at different concentrations. (C) Detailed structure of a DRAST chip well. Each test well consists of a micropatterned radial chamber for agarose matrix molding and a satellite well for freeze-dried antimicrobials. Inset images show the micropatterned chamber i) before agarose mixture loading and ii) after agarose mixture loading. (D) Experimental process for detecting bacteria in blood. A sample from a PBCB is mixed with agarose and loaded into the loading chamber in the chip. Freeze-dried antibiotics are rehydrated by adding culture media. Automated microscopic imaging is used to detect the growth of pathogens. Inset scanning electron microscope (SEM) images show i) freeze-dried antibiotics in the satellite well and ii) the focus mark on the bottom of the chip for automated imaging. (E) In the initial state, pathogens were not detectable using a 20x magnification lens; only blood cells were detectable. After four hours of incubation, in the case of resistance to the antibiotic, a single bacterium divided and formed a microcolony. Filled triangle represents a blood cell. Unfilled triangle represents a bacterial microcolony. The scale bar represents 10 mm in (B), 3 mm in (C), 300  $\mu\text{m}$  in (D), and 100  $\mu\text{m}$  in (E). (Reprinted from [11])

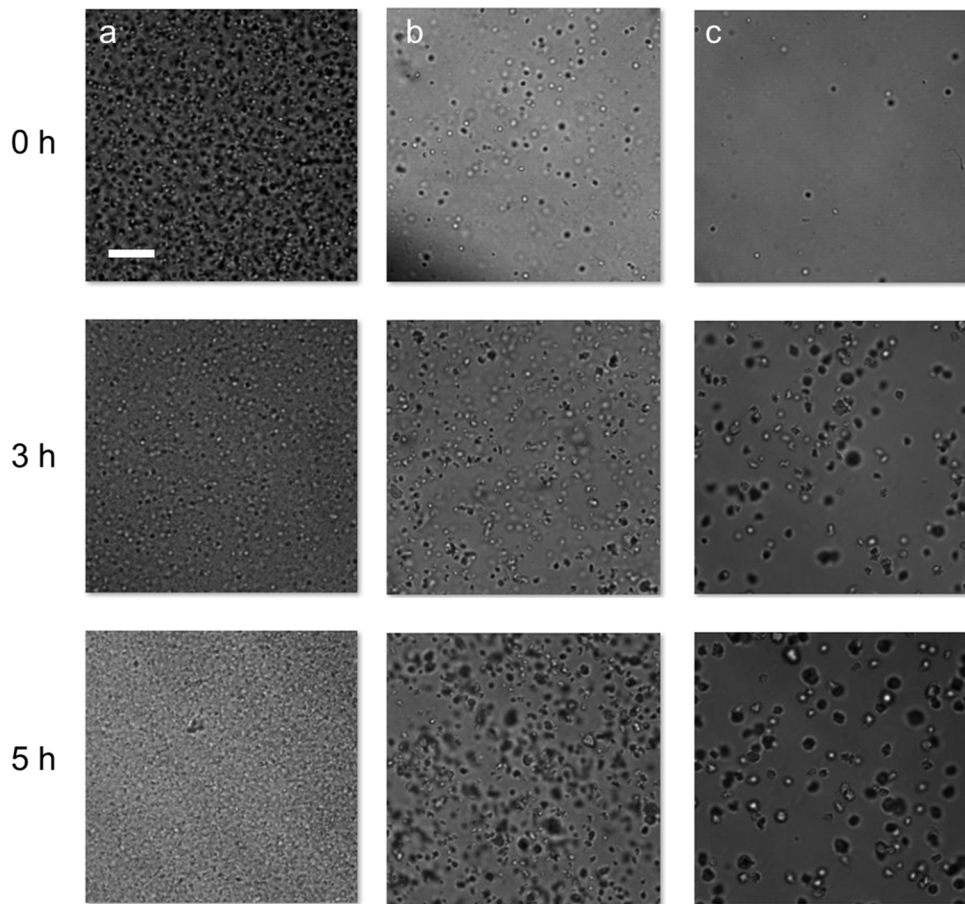


Figure 2.2 Time-lapse images of colonies from different dilution factors. (a) The raw sample from the PBCB was mixed with agarose. (b) A 10x dilution sample from PBCB. (c) A 100x dilution sample from PBCB. The scale bar represents 100  $\mu\text{m}$ . (Reprinted from [11])

Antimicrobial	MIC, dRAST (µg/ml)	MIC, BMD (µg/ml)	CLSI QC range (µg/ml)	MIC, dRAST (µg/ml)	MIC, BMD (µg/ml)	CLSI QC range (µg/ml)
<b>(A) Gram-negative strains</b>						
<i>E. coli</i> ATCC 25922			<i>P. aeruginosa</i> ATCC 27853			
Amikacin	2,4	2,4	0.5-4	2	1-4	1-4
Amoxicillin/ clavulanic acid	8/4	8/4	2/1-8/4	-	-	-
Aztreonam	0.25	0.12-0.5	0.06-0.25	4	2,4	2-8
Cefepime	0.06, 0.12	0.03, 0.12	0.015-0.12	2	1,2	0.5-4
Cefotaxime	-	-	-	32	16	8-32
Ceftazidime	-	-	-	2,4	2	1-4
Ciprofloxacin	-	-	-	0.25,0.5	0.25,0.5	0.25-1
Colistin	2	0.5,1	0.25-2	2,4	1	0.5-4
Fosfomycin	-	-	-	2,4	8	2-8
Gentamicin	1	0.25-1	0.25-1	1,2	1,2	0.5-2
Imipenem	-	-	-	2,4	4	1-4
Meropenem	-	-	-	0.5,1	0.5	0.25-1
Piperacillin	4	4	1-4	4,8	4	1-8
Piperacillin/ tazobactam	4/4	2/4,4/4	1/4-4/4	8/4	8/4	1/4-8/4
Trimethoprim/ sulfamethoxazole	≤0.5/9.5	≤0.5/9.5	≤0.5/9.5	-	-	-
Ticarcillin	16	8,16	4-16	16,32	16,32	8-32
Ticarcillin/ clavulanic acid	4/2	8/2, 16/2	4/2-16/2	-	-	-
Tobramycin	1	0.5,1	0.25-1	0.5,1	0.25,0.5	0.25-1
<b>(B) Gram-positive strains</b>						
<i>S. aureus</i> ATCC 29213			<i>E. faecalis</i> ATCC 29212			
Ampicillin	1	1,2	0.5-2	2	2	0.5-2
Ciprofloxacin	0.12,0.25	0.25,0.5	0.12-0.5	2	2	0.25-2
Clindamycin	0.12,0.25	0.12, 0.25	0.06-0.25	8,16	8, 16	4-16
Erythromycin	0.25, 0.5	0.5	0.25-1	2	1, 2	1-4
Gentamicin	0.5	0.25, 0.5	0.12-1	4	8	4-16
Imipenem	-	-	-	1,2	2	0.5-2
Levofloxacin	0.25	0.25	0.06-0.5	0.5	0.5, 1	0.25-2
Linezolid	1	4	1-4	1,2	2	1-4
Oxacillin	0.5	0.25, 0.5	0.12-0.5	16	8,16	8-32
Penicillin	0.5	0.5,1	0.25-2	2	2	1-4
Rifampin	-	-	-	1	1,2	0.5-4
Tetracycline	0.25,0.5	0.5,1	0.12-1	8	16,32	8-32
Trimethoprim/ sulfamethoxazole	≤0.5/9.5	≤0.5/9.5	≤0.5/9.5	≤0.5/9.5	≤0.5/9.5	≤0.5/9.5
Vancomycin	1	1,2	0.5-2	2,4	4	1-4

Table 2.1 MIC values from DRAST with spiked sample, broth microdilution test and CLSI quality control ranges. The DRAST test was performed on a positive blood culture sample spiked with four standard strains. The broth microdilution test

was performed on a colony cultured on an LB agar plate. Each test was performed in three times. (Reprinted from [11])

### **2.1.3. DRAST validation with spike-in sample**

Four standard CLSI pathogen strains – *E. coli* ATCC 25922, *S. aureus* ATCC 29213, *P. aeruginosa* ATCC 27853, and *E. faecalis* ATCC 29212 - were cultured on Luria-Bertani (LB) agar plates. Then, 100 µl of bacterial solution containing approximately 10 CFU of bacteria was inoculated into blood culture bottles. To each bottle, 8 ml of fresh human blood from healthy volunteers was added to mimic blood culture bottles. The spiked blood culture bottles were incubated in automated blood culture machines. After the positive signal from PBCB, sampling was performed for DRAST. Briefly, 10 µl of sample was diluted with 990 µl of culture media, and 300 µl of the diluted sample was mixed with 900 µl of 0.5% agarose. Then, 10 µl of the mixture was inoculated into a micropatterned chamber in DRAST chip. Time-lapse imaging was performed every 2 hours.

### **2.1.4. Positive blood culture bottles**

For positive blood culture, BACTEC blood culture bottles that were flagged as positive for microbial growth by a BACTEC FX automated incubation system (Becton Dickinson Company, NJ, United States) and BacT/Alert FA Plus and SN bottles in a BacT/Alert® 3D system (bioMérieux Inc., Marcy l'Étoile, France) were subjected to parallel testing using DRAST and the conventional broth dilution test.

Samples of PBCBs flagged as positive during the over-night culture period were used. All samples from which a single bacterial species determined by Gram staining, recovered by conventional processing were included in a comparative analysis of the identification results. PBCBs were supplied by Seoul National University Hospital (SNUH). Pure cultures of the clinical strains from PBCBs were inoculated on Luria-Bertani (LB) agar plates (BD Biosciences, CA, United States) and incubated for 20 to 24 hours. After incubation, colonies were used to prepare bacterial stocks at a concentration of  $1.5 \times 10^8$  CFU/ml. Bacterial identification was performed by following the protocols of the hospital where the strain originated: Gram-negative strains were identified by VITEK ID-GN cards in Vitek2 Systems (bioMerieux Inc., Marcy l'Étoile, France) and Gram-positive strains by Pos Breakpoint Combo Panel Type 28 in MicroScan (Beckman Coulter Inc., CA, United States) at SNUH.

#### **2.1.5. The number of bacteria in PBCBs**

DRAST system processes a wide dynamic range of inoculum sizes from positive blood culture bottles (PBCBs) without prior preparation. As DRAST system utilizes positive blood culture bottles, it is of high importance to find out the number of pathogens inside PBCBs. The number of bacteria in a PBCB is the must-know information for the determination of the dilution factor. Conventional blood culture bottles detect the CO<sub>2</sub> generated from bacteria, which does not

precisely represent bacterial population in the culture bottle. To find out the number of pathogens in a PBCB, we performed conventional microbiological quantification method, a colony forming unit (CFU) detection. After dilution of PBCB samples with culture media by  $10^6$  fold, 100  $\mu$ l of diluted sample was inoculated onto solid media. After counting the colonies formed, the estimation of the number of pathogens was done as shown below. (Figure 2.3)

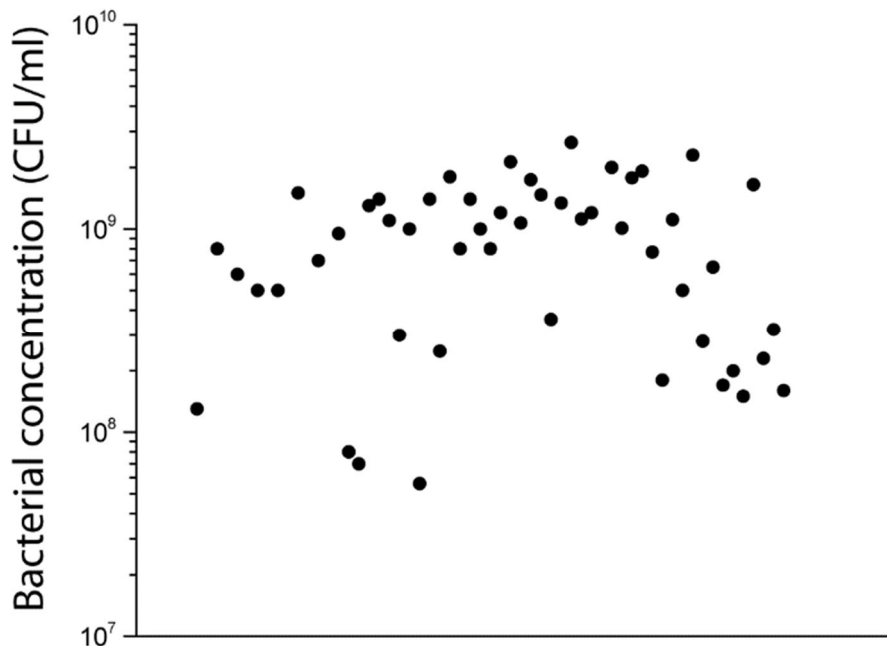


Figure 2.3 Number of bacterial pathogens in PBCBs. The average number of pathogens was about  $9.4 \times 10^8$  CFU/ml. The highest concentration was about  $2.5 \times 10^9$  CFU/ml, and the lowest was about  $5.6 \times 10^7$  CFU/ml. (Reprinted from [11])

### 2.1.6. Image acquisition in DRAST

For the detection of bacteria, magnification higher than 400x is necessary. However, in this system, a bacterial microcolony is imaged rather than a single bacterium. Therefore, relatively low 100x magnification imaging (a 20x lens with a 5x tube lens or a 10x lens with a 10x tube lens) was used. The 96-well format DRAST chip was scanned, and each well in the chip was imaged in a custom-made automated imaging system. The imaging system consisted of an xy-axis motor (Ezi-Step-42S, Fastech, Inc., Republic of Korea) with a motion controller (DMC-

B140, Galli Motion Control, Rocklin, CA, United States), a z-axis motor (SAN4505-150PR+3SR, Sciencetown, Inc., Republic of Korea) with a motion controller (PMC-1HS, Autonics Sensors & Controllers, Republic of Korea), a CMOS camera (Ximea, USB3 Vision xiQ MQ022CG-CM, Münster, Germany), a 20x objective lens (Olympus, UPlanFL N, Tokyo, Japan), and related electronics. The automated operation of the system was controlled using in-house-developed PC software. Predefined wells in the chip, divided based on antibiotic panel type (Gram-positive and Gram-negative), were scanned automatically to obtain images of microcolonies. To find an imaging area in each well and an identical imaging plane in the z-axis across all wells with different vertical profiles, we used a focus mark injection-molded as a half-cross shape on the bottom of each well. The image was processed to find the position and contrast of the focus mark while vertically scanning the well bottom. The z-axis reference position that produced the greatest contrast of the focus mark image was obtained by vertically scanning the well bottom (first coarse scan range/step: 468.75/46.87  $\mu\text{m}$ , second fine scan range/step: 112.5/5.62  $\mu\text{m}$ ). At the same time, the xy reference position was obtained from the position of the mark in the image found by pattern-matching of the half-cross shape. Finally, the microcolony image was acquired after moving the xyz stage by the amount of the predefined offsets.

### 2.1.7. Colony formation monitoring

Colony formation in the DRAST chip was monitored by a QMAP (QuantaMatrix microscopic analysis platform) automated image analyzer with a total magnification of 100x using a 20x lens and a 5x tube lens. The imaging area was 1126.4  $\mu\text{m}$  x 594  $\mu\text{m}$ . Time-lapse images were acquired in the same area.

## 2.2. Design and fabrication of DRAST chip

### 2.2.1. Diffusion limit and gradient generation

Previously, our group proposed rapid AST based on pathogen immobilization inside agarose matrix and following time-lapse imaging with single cell morphological analysis (SCMA) as shown in the following figure. (Figure 2.4)

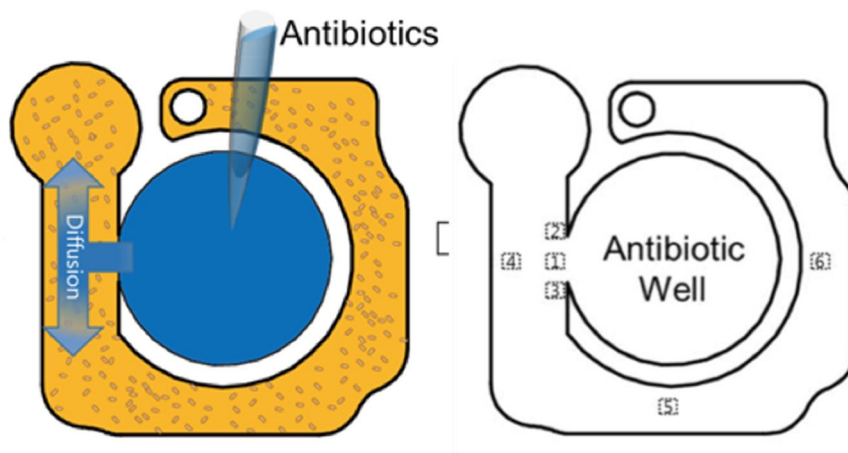


Figure 2.4 The schematic figures of loading antimicrobials into agarose matrix in

previous MAC chip (Reprinted from [24])

Due to the design of previous 96-well format MAC chip, there a concentration gradient of antimicrobials occurred across the agarose matrix. The results due to concentration gradient could be seen from Figure 2.5 and Figure 2.6.

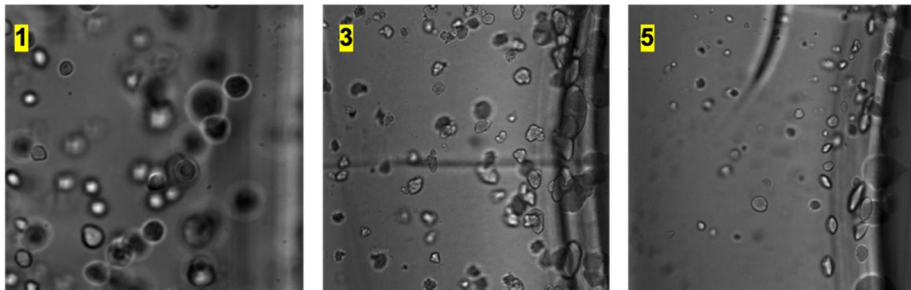


Figure 2.5 Images of bacteria inside the agarose matrix in different regions without antibiotics after 6 hours of incubation. The growth difference can be easily detected. (Reprinted from [24])

In regions 5 and 6, the bacteria divided regardless of antimicrobial concentration. However, our group constantly took images from region 1 with 40x microscopic lens, where the closest region from antimicrobial well, the AST results were fine with reference method.

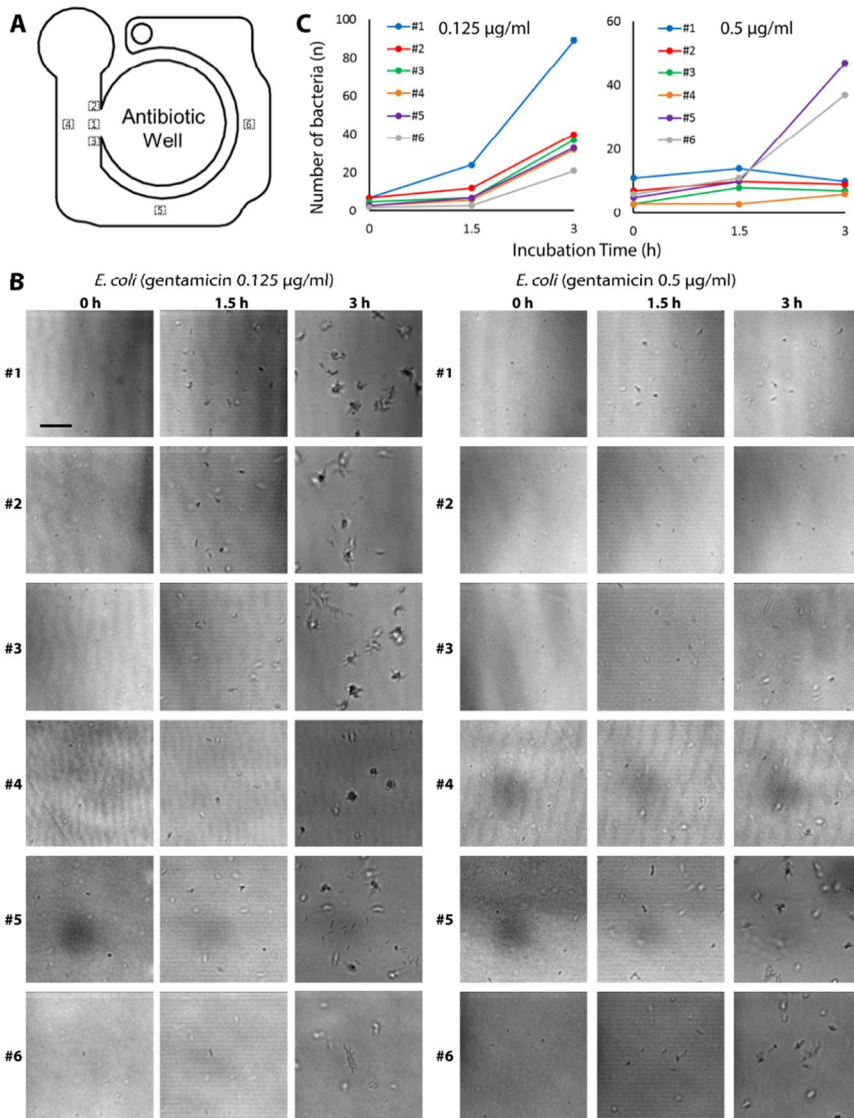


Figure 2.6 (A) The six different imaging regions. (B) Time-lapse images of *E. coli* treated with gentamicin at two different concentrations at the different locations. In regions 1–4, near the antibiotic well, the responses of the bacteria were identical. In regions 5 and 6, the bacteria divided regardless of antibiotic concentration. Scale bar, 25 µm. (C) The number of bacteria according to the each region in (B).

(Reprinted from [24])

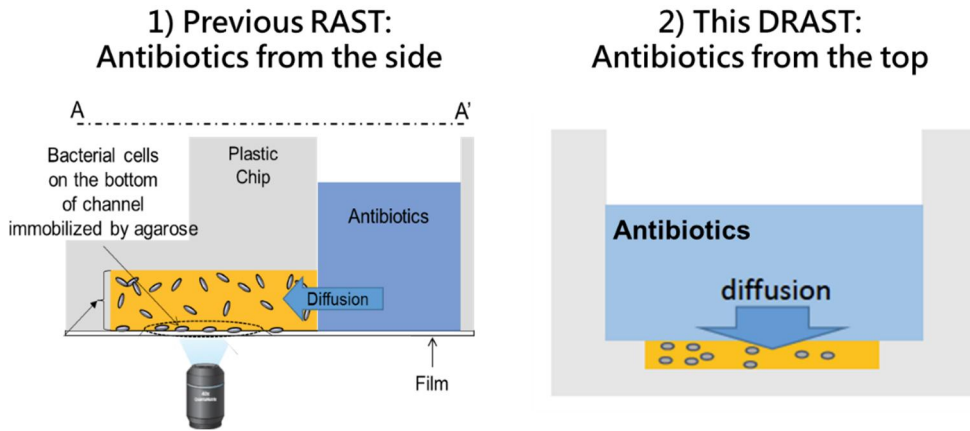


Figure 2.7 The comparative schematic figures of the diffusion approach between previous MAC chip and DRAST chip [11, 24]

However, in DRAST system, as we planned to take larger images with lower magnification lens (10x), there should be none of the concentration gradient of antimicrobials over the agarose matrix. Thus, we decided to employ another diffusion approach rather than lateral diffusion previously employed. We fabricated the prototype DRAST chip of poly (methyl methacrylate) (PMMA) with computer numerical control (CNC) machines. The 300  $\mu\text{m}$  and 500  $\mu\text{m}$  sized concentric circle was located at the center of microwells. As shown in Figure 2.8, the agarose matrix with color dyes was stable after loading of phosphate buffered saline (PBS) for prototyping. After prototyping with color dyes and PBS, we loaded the mixture of agarose matrix pathogens with subsequent loading of culture media. The bacterial growth was confirmed over the one week of incubation.

### Initial prototype for DRAST chip

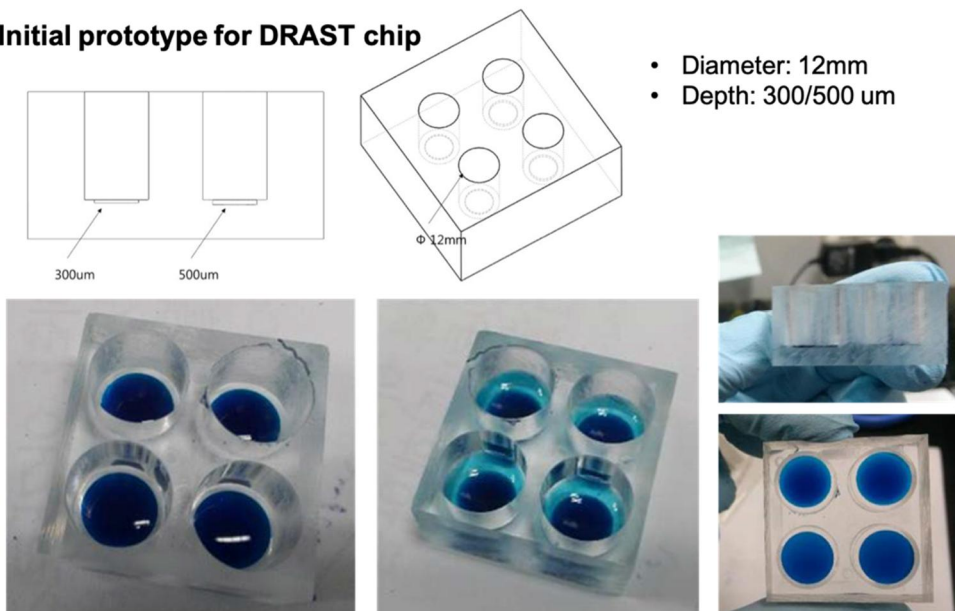


Figure 2.8 The schematic design of initial prototype for DRAST chip.

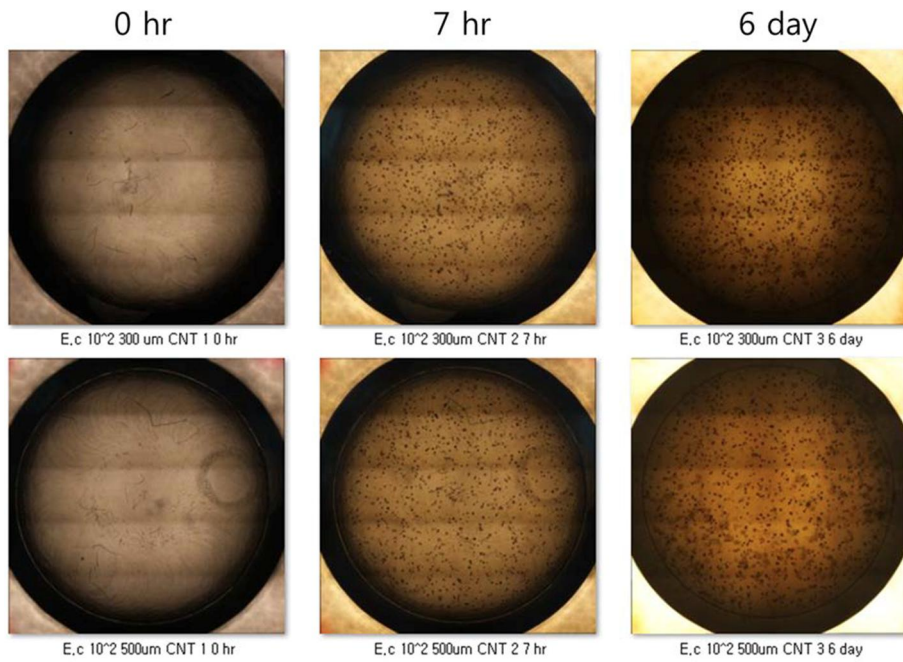


Figure 2.9 Time-lapse images in DRAST prototype (Figure 2.8) PMMA chip



Figure 2.10 The design candidates of DRAST chip for stable loading agarose matrix

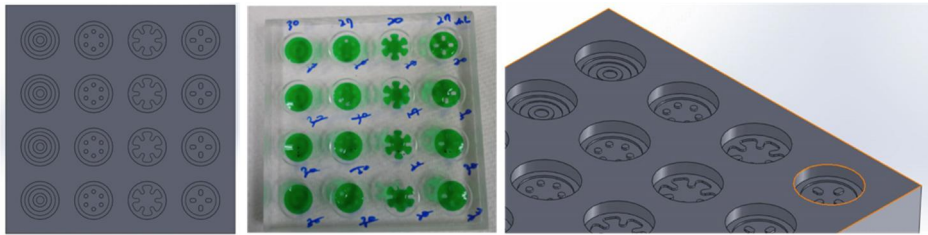


Figure 2.11 Images of top and perspective view and prototype of various designs

For the most stable loading of agarose matrix, various design as shown above, had been considered based on design parameters including surface area, overall capacity, well capacity, volume of over-well, height of over-well and height from the bottom. Overall, the total thickness of agarose matrix was 700 ~ 800  $\mu\text{m}$ . From the previous study, the diffusion of antimicrobials was guaranteed in 500  $\mu\text{m}$  from source. Additionally, if the agarose matrix is thicker than 500  $\mu\text{m}$ , the growth of bacteria at the bottom could be inhibited or delayed due to the limitation of oxygen and nutrient. The main well design is decided after the considering the specific parameters of 4 design candidates. (Figure 2.9, Figure 2.10, Figure 2.11) From 4 designs, design 1 was most stable for loading agarose matrix after having a number of tests. In contrast to previous rapid AST reported by our group, DRAST chip should be designed to utilize another diffusion from the side as mentioned earlier. To accomplish this, we devised the satellite well connected to the main concentric-shaped micropatterned chamber. This satellite well is used for the storage of lyophilized antimicrobials as mentioned in the previous section. To prevent the early diffusion of dissolved antimicrobials between the satellite well and the main

chamber, the bumper has been designed.

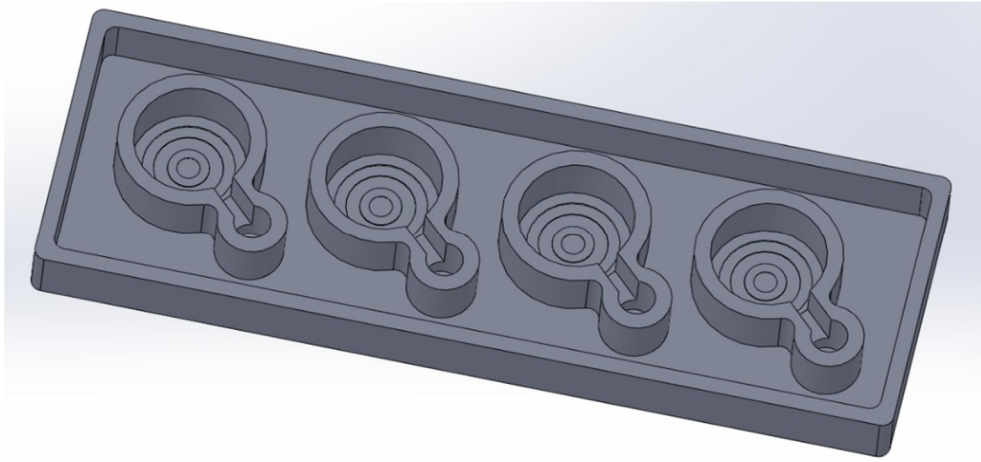


Figure 2.12 The perspective view of DRAST chip consists of 4 main chambers with connected the satellite well

After the design of the DRAST chip, the validation test of DRAST chip composed of the growth confirmation and AST profiling, this design passed the two tests. The lyophilized form of antimicrobials can be loaded in the satellite well. The satellite well size was enough to fit the size of commercial beads. After the whole design and validation works, this micropatterned chamber with the satellite well was re-designed in the form of 96-well format for high-throughput as there needs various kinds of antimicrobials and concentrations for AST. The complete design of DRAST chip in 96-well format can be found in Figure 2.1.

### **2.2.2. Application of lyophilization for DRAST chip**

For easier handling of DRAST procedures, we applied the lyophilization

of antimicrobials [34]. The antimicrobials which were prepared prior to DRAST tests, were freeze-dried in the DRAST chip and broth micro dilution plates for immediate testing. The antimicrobial was prepared at a 10-fold higher concentration than the actual test concentrations to be tested. Then, 10  $\mu$ l of concentrated antimicrobial was loaded into the satellite well in the DRAST chip. For lyophilization, a PVTFD 10R programmable vacuum freeze dryer (Ilshin Lab, Kyunggi-Do, Republic of Korea) was used. The freeze-drying process involved a freezing tray, freezing trap, vacuum and heating tray. (Figure 2.13) The heating process during the freeze-drying process is shown below. (Table 2.2) After freeze-drying process, the DRAST chip was stored at 4 °C with desiccating agent.

	Sequence #1	Sequence #2	Sequence #3	Sequence #4	Sequence #5	Sequence #6
Temp (°C)	-40	-20	-10	0	10	20
Vac (mTorr)	0	0	0	0	0	0
Set Time (Min)	60	60	60	60	60	$\infty$

Table 2.2 The heating process during the freeze-drying process. After freezing tray, freezing trap and vacuum process in freeze-drying, the tray was heated for decrease the water content in antibiotics. The heating process was composed of several sequences

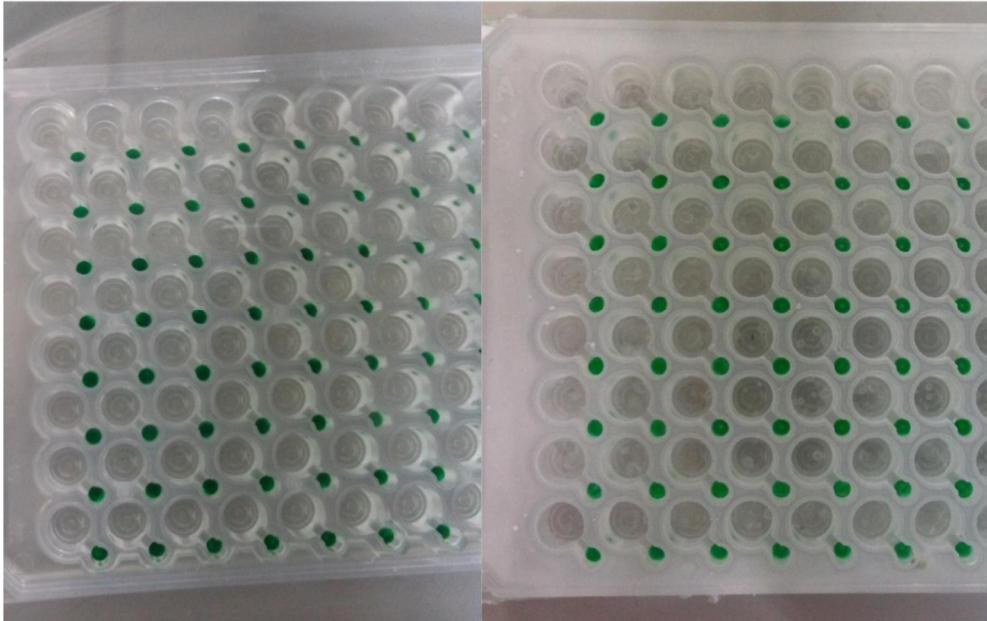


Figure 2.13 The results of food dye solution after freeze-dry process

### 2.3. DRAST system as an inoculum effect free system

#### 2.3.1. Inoculum effect

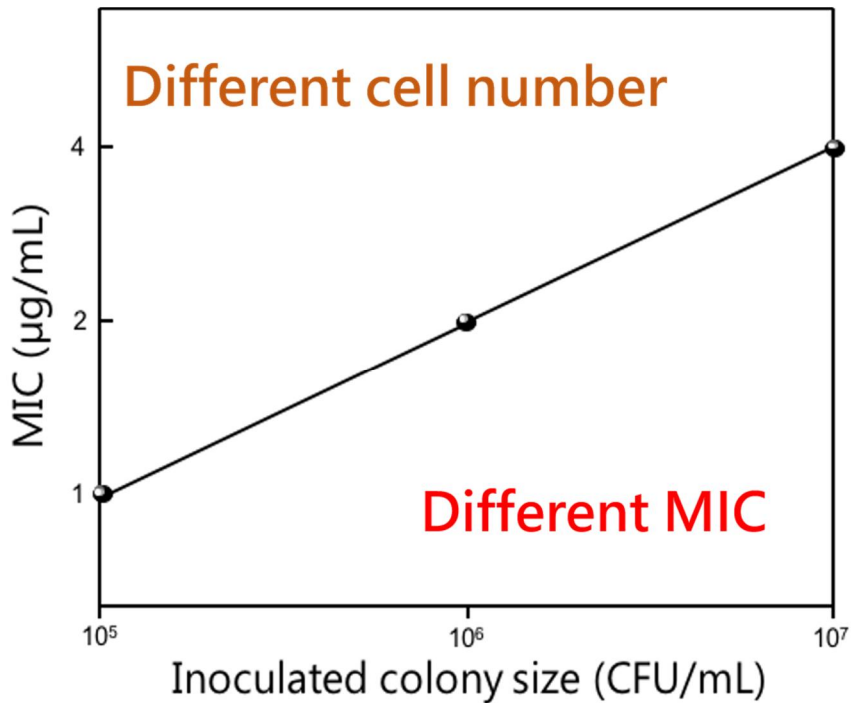


Figure 2.14 The illustrated figure of the example of inoculum effect

The inoculum effect (IE) is a laboratory phenomenon which is as a significant increase in the MIC of an antimicrobials when the number of microorganisms inoculated is increased [35]. As DRAST system is designed to utilize the PBCBs after positive blood culture signal, this system should prove itself to be free from this IE. The results of IE-free validation of DRAST system will be discussed afterwards.

### **2.3.2. The validation of DRAST system to be no inoculum effect**

Conventional turbidity-based AST systems necessitate a precise bacterial inoculum size in the test well for accurate AST results [36]. Therefore, another obstacle to demonstrate direct AST from PBCBs derives from the fact that the bacterial concentration inside PBCBs has a wide range and cannot be measured by the current culture detection instrument. The measurement of the bacterial concentrations of PBCBs was done by the observation of colony formation on Luria-Bertani (LB) agar plates and found that the concentrations ranged widely, from  $5.6 \times 10^7$  to  $2.6 \times 10^9$  CFU/ml. (Figure 2.3) In the DRAST system, we diluted the PBCB sample at a 1:100 volume ratio, resulting in bacterial concentrations from approximately  $5.0 \times 10^5$  to  $5.0 \times 10^7$  CFU/ml. The DRAST system should produce identical AST results from this diluted inoculum range. To validate that the DRAST system could perform reliably at this wide range of inoculum sizes, we tested four standard strains, *E. coli* ATCC 25922, *P. aeruginosa* ATCC 27853, *S. aureus* ATCC 29213 and *E. faecalis* ATCC 29212, at inoculum sizes of  $5.0 \times 10^5$ ,  $5.0 \times 10^6$  and  $5.0 \times 10^7$  CFU/ml. The validation concentrations were determined based on the bacterial concentrations measured in the PBCBs. *E. coli* ATCC 25922 at three inoculum sizes –  $5.0 \times 10^5$ ,  $5.0 \times 10^6$  and  $5.0 \times 10^7$  CFU/ml – was imaged after four hours of incubation with or without antimicrobial (gentamicin). (Figure 2.15)

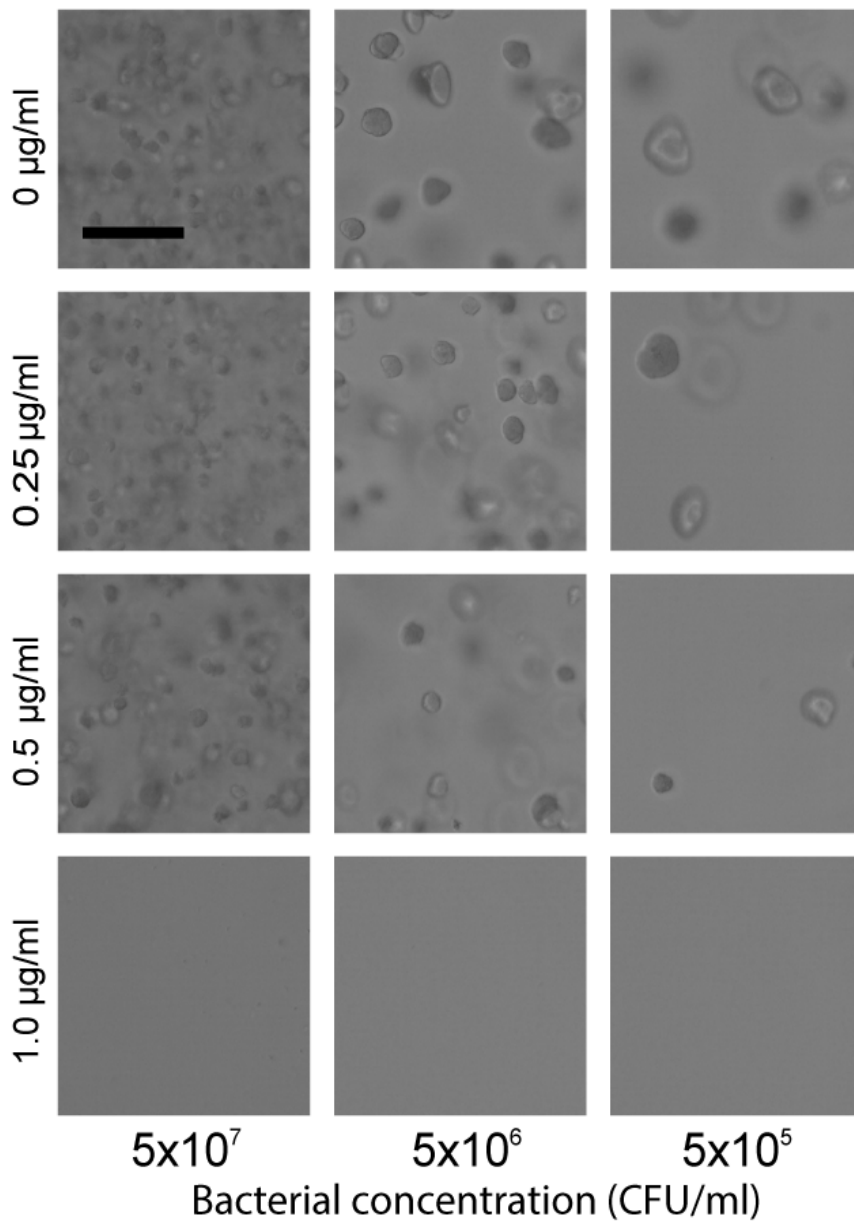


Figure 2.15 Colony formation of bacteria at different inoculum sizes. In all inoculum sizes from  $5.0 \times 10^7$  to  $5.0 \times 10^5$  CFU/ml, there was microcolony

formation at 0, 0.25 and 0.5  $\mu\text{g/ml}$  gentamicin. At 1  $\mu\text{g/ml}$  gentamicin, there was no colony formation at any inoculum size. The scale bar represents 100  $\mu\text{m}$ . (Reprinted from [11])

In the absence of antimicrobials, bacterial colonies formed at all the inoculum sizes. There were approximately 10~1,000 bacterial cells in the whole image view (1126.4 x 594  $\mu\text{m}$ ). (Table 2.3)

	Number of bacteria (CFU)				In FOV of 20x lens
	1 ml of positive blood culture bottle	1 ml of 100x dilution	1 ml of mixture with agarose	10 $\mu\text{l}$ of mixture in the well	
<b>Average</b>	$9.4 \times 10^8$	$9.4 \times 10^6$	$2.3 \times 10^5$	$2.3 \times 10^4$	160
<b>Min</b>	$5.6 \times 10^7$	$5.6 \times 10^5$	$1.4 \times 10^5$	$1.4 \times 10^3$	10
<b>Max</b>	$2.6 \times 10^9$	$2.6 \times 10^7$	$6.5 \times 10^6$	$6.5 \times 10^4$	460

Table 2.3 Number of bacteria in the well and field of view (FOV). We diluted the PBCBs by 1/100. On average, the final concentration was  $9.4 \times 10^6$  CFU/ml. After mixing with agarose at a 1:3 volume ratio, the concentration was  $2.3 \times 10^6$  CFU/ml. In this case, the final concentration in the well was  $2 \times 10^4$  CFU, and there were approximately 100 bacteria cells in the field of view of the 20X lens with a 5x tube lens. (Reprinted from [11])

The size of the colony in images varied according to the inoculum size. (Figure 2.15) We assumed that this variation of bacterial colony size was due to quorum sensing in the bacteria; at high densities, bacteria produce and release chemical signal molecules to control cell density [37, 38]. Inoculum size showed an inverse relationship with colony size. At all the inoculum sizes, colonies were observed after incubation with gentamicin at concentrations below 0.5  $\mu\text{g/ml}$ ;

however, no colonies were observed when 1  $\mu\text{g/ml}$  gentamicin was applied. We tested 17 clinically important antimicrobials with *E. coli* ATCC 25922 in the same range of inoculum sizes and compared the MIC values at each inoculum size. (Figure 2.16 and Figure 2.17)

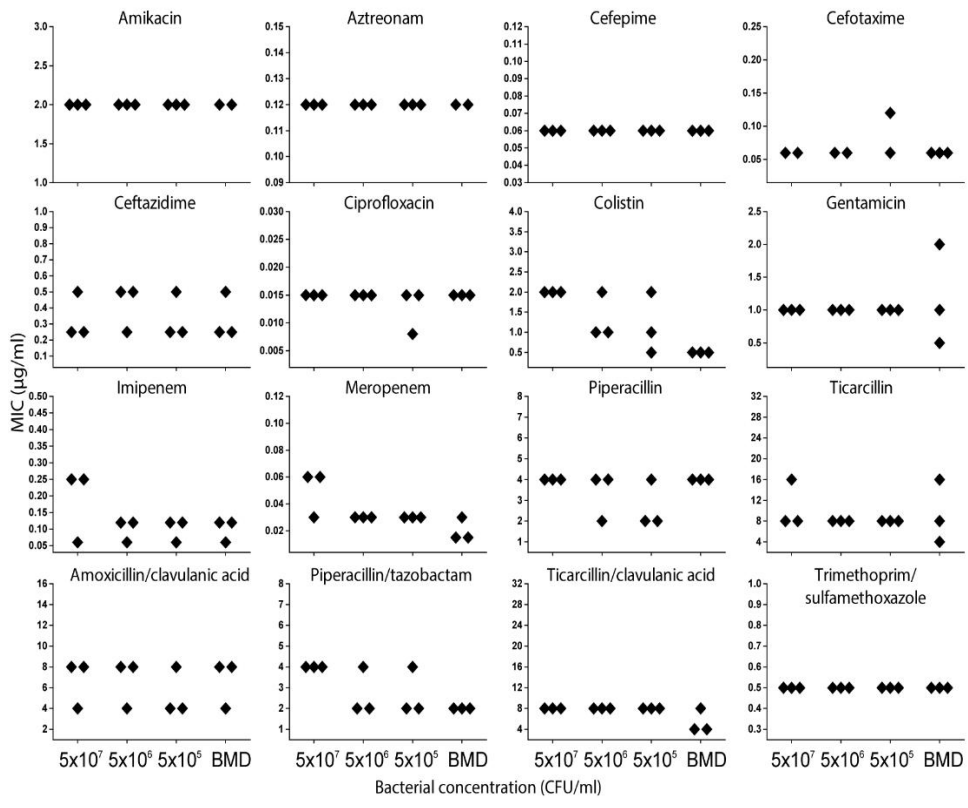


Figure 2.16 MIC values from different *E. coli* ATCC 25922 inoculum sizes of  $5.0 \times 10^7$ ,  $5.0 \times 10^6$  and  $5.0 \times 10^5$  CFU/ml incubated with 17 clinically important antimicrobials and analyzed using DRAST and broth microdilution test. For all inoculum sizes, the MIC values were in the middle of the CLSI quality control ranges. (Reprinted from [11])

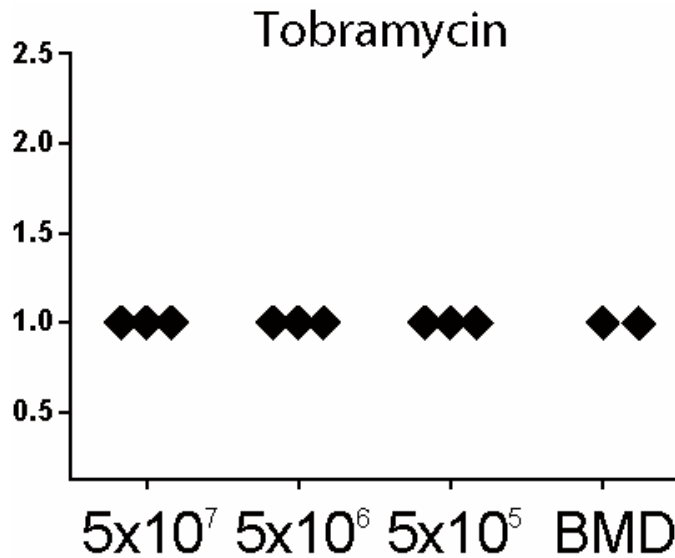


Figure 2.17 Consistent AST results from a wide range of inoculum sizes. MIC values from different *E. coli* ATCC 25922 inoculum sizes of  $5.0 \times 10^7$ ,  $5.0 \times 10^6$  and  $5.0 \times 10^5$  CFU/ml incubated with tobramycin and analyzed using DRAST and broth microdilution test. (Reprinted from [11])

There were 30 cases of a two-fold difference at all inoculum sizes and one case in which the MIC value showed two two-fold differences, at  $5.0 \times 10^5$  and  $5.0 \times 10^7$  CFU/ml, resulting in a 99.33% essential agreement rate. (Table. 2.4)

Bacterial concentration (CFU/ml)	<i>E. coli</i> ATCC 25922			<i>P. aeruginosa</i> ATCC 27853		
	Correct	One two-fold	Two two-fold	Correct	One two-fold	Two two-fold
5x10 <sup>7</sup> vs 5x10 <sup>6</sup>	39	11	0	32	16	0
5x10 <sup>7</sup> vs 5x10 <sup>5</sup>	36	13	1	33	15	0
5x10 <sup>6</sup> vs 5x10 <sup>5</sup>	44	6	0	37	11	0
<b>Total</b>	<b>119</b>	<b>30</b>	<b>1</b>	<b>102</b>	<b>42</b>	<b>0</b>
<b>Essential agreement</b>	<b>99.33 %</b>			<b>100 %</b>		
<b>Categorical agreement</b>	<b>100 %</b>			<b>95.24 %</b>		

Bacterial concentration (CFU/ml)	<i>S. aureus</i> ATCC 29213			<i>E. faecalis</i> ATCC 29212		
	Correct	One two-fold	Two two-fold	Correct	One two-fold	Two two-fold
5x10 <sup>7</sup> vs 5x10 <sup>6</sup>	22	13	1	28	7	0
5x10 <sup>7</sup> vs 5x10 <sup>5</sup>	17	15	4	28	7	0
5x10 <sup>6</sup> vs 5x10 <sup>5</sup>	28	8	0	33	2	0
<b>Total</b>	<b>67</b>	<b>36</b>	<b>5</b>	<b>89</b>	<b>16</b>	<b>0</b>
<b>Essential agreement</b>	<b>95.37 %</b>			<b>100 %</b>		
<b>Categorical agreement</b>	<b>100 %</b>			<b>100 %</b>		

Table 2.4 Summary of a comparison of AST results from various inoculum sizes of *E. coli* ATCC 25922, *P. aeruginosa* ATCC 27853, *S. aureus* ATCC 29213 and *E. faecalis* ATCC 29212. “Correct” means a case with identical MIC values from different inoculum sizes. “One two-fold” and “Two two-fold” denote cases with MIC values from different inoculum sizes that were different by two-fold and four-fold, respectively. “Essential agreement” refers to the proportion of cases that were correct or had one two-fold difference. The essential agreement rates were 99.33% in *E. coli* ATCC 25922, 100% in *P. aeruginosa* ATCC 27853, 95.37% in *S. aureus* ATCC 29213 and 100% in *E. faecalis* ATCC 29212. (Reprinted from [11])

We performed the same test by applying various antimicrobials to *P. aeruginosa* ATCC 27853, *S. aureus* ATCC 29213 and *E. faecalis* ATCC 29212, and the essential agreement rates were 100%, 95.37% and 100%, respectively. We were able to conclude that inoculum size did not have a significant effect on the AST results in DRAST system. The DRAST system was able to detect a wide range of bacterial concentrations with no difference in AST results, encompassing almost all PBCB concentrations with a dynamic range from  $5 \times 10^7$  to  $5 \times 10^9$  CFU/ml. It has been established that in AST, MICs tend to increase at inoculum sizes larger than the standard ( $5 \times 10^5$  CFU/ml)[39-42]. However, the DRAST system was free of this phenomenon even at the high concentration of  $5 \times 10^9$  CFU/ml. In the DRAST system, the PBCB is diluted 100-fold with culture media and mixed with agarose at a 1:3 volume ratio; then, only 10  $\mu$ l of the mixture is added to the well. Therefore, the final concentration of bacteria in the well is  $1.25 \times 10^6$  CFU/ml, only a two-fold difference from the standard inoculum. At the low inoculum size of  $5 \times 10^7$  CFU/ml, the final concentration of bacteria in the well is  $1.25 \times 10^4$  CFU/ml, which might make it difficult to detect bacterial growth. However, the DRAST system involves observations of microcolony formation from a single bacterium in agarose; this low limit of detection allows accurate MIC determination at low concentrations.

#### **2.4. Automatic AST using microcolony-forming area detection using image processing algorithm**

Clinical use of the DRAST system needs an automated system of time-lapse imaging through the final AST result. In DRAST system, raw images were obtained from the prepared micropatterned DRAST chip with an automated image acquisition system using a time-lapse method. (Figure 2.18A) For example, a clinical strain, *K. pneumoniae*, was tested with amoxicillin/clavulanic acid (A/C) for the determination of MIC. Raw images were automatically analyzed to determine the MIC from serial dilution tests with antibiotics. The main role of this program is to calculate the area of colony formation in the images, which is accomplished by calculating the area occupied by bacteria. The raw images were transformed into a binary format through several processes. (Figure 2.18 and Figure 2.19)

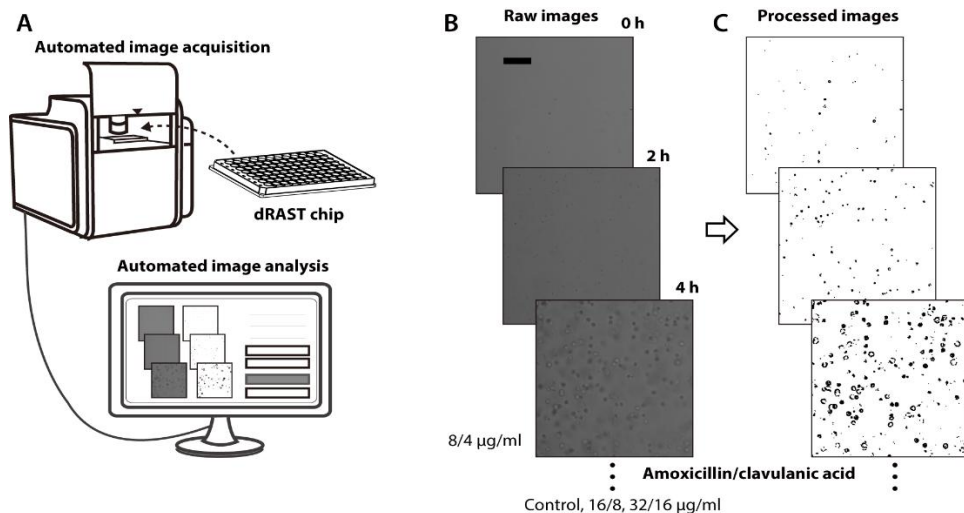


Figure 2.18 (A) Time-lapse images were acquired from the automated imaging system, and the image data were transferred to the analysis system. (B) Time-lapse

images of *K. pneumoniae* with several concentrations of amoxicillin/clavulanic acid (A/C). (C) The raw images from (B) were processed to binary format images. The number of white pixels in the image represents the microcolony area. The scale bars in (B) represent 100  $\mu\text{m}$ . (Reprinted from [11])

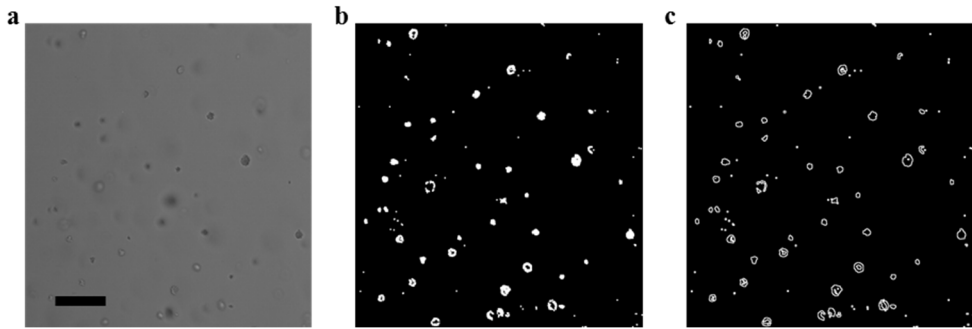


Figure 2.19 Image processing for microcolony detection. (a) The raw image acquired from the imaging system. (b) The result of sharpening and binarization. (c) The detected contours of the microcolonies recognized in (b). The scale bar represents 300  $\mu\text{m}$  (Reprinted from [11])

After the area in the binary format image was calculated, a growth curve was generated. (Figure 2.20A) The initial images sometimes contained blood cells or some debris. To compensate for this debris, the growth rate of the colony formation area was calculated as in eqn. 1.

$$A_{S,N} = \frac{A_{S,F} - A_{S,I}}{A_{C,F} - A_{C,I}} \quad (\text{eqn. 1})$$

where  $S$  and  $C$  represent the sample and control, respectively;  $F$  and  $I$  represent the final and initial times of the image, respectively; and  $A_{S,N}$  represents the normalized growth rate of the area of a sample microcolony in the images. To determine MIC, a distinction between growth and non-growth is needed, which requires a threshold value. In broth microdilution (BMD) test, the MIC is the lowest concentration of antimicrobial agent that completely inhibits growth of the organism in microdilution wells as detected by the unaided eye [43].

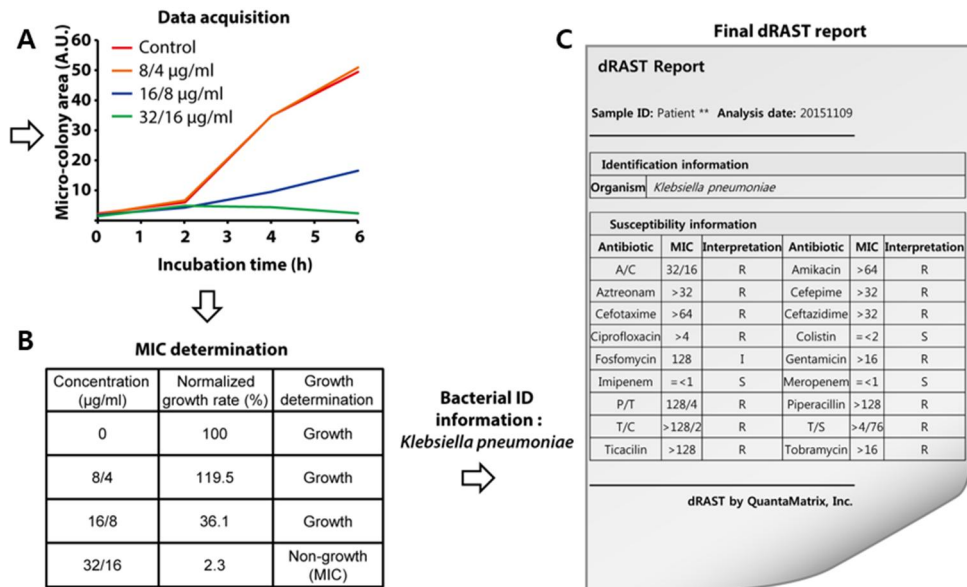


Figure 2.20 (A) Graph of the microcolony-forming area in Figure 2.19C. From low A/C concentrations until 16/8 µg/ml, there was a substantial increase in microcolony-forming area in the images. However, from 16/8 µg/ml to 32/16 µg/ml, there was no substantial change in the area of bacteria. (B) The normalized growth rates at all the concentrations were calculated. Values higher than 20% were

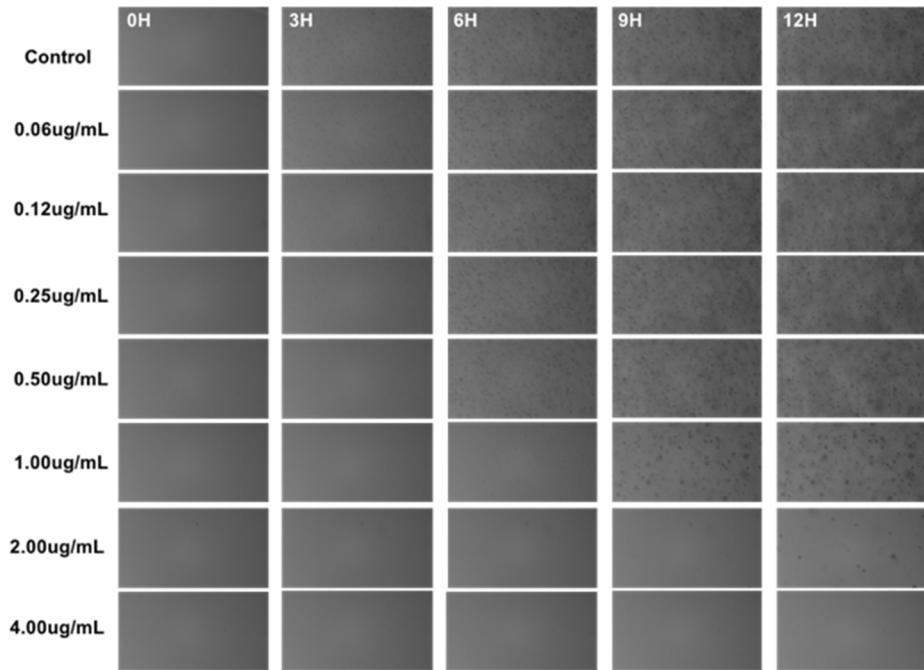
regarded as growth, and lower values were regarded as non-growth. From low A/C concentrations until 16/8 µg/ml, the normalized growth rates were higher than 20% and regarded as growth. However, at 32/16 µg/ml, the normalized growth rate was 2.3% and lower than 20%; thus, it was regarded as non-growth. Therefore, the MIC value was determined to be 32/16 µg/ml. (C) Final AST report. Using the ID information and MIC interpretive criteria from CLSI, antibiotic susceptibility was determined in a full antimicrobial panel.

However, the imaging method detected some growth at high concentrations that was not detected using the BMD method. We performed a spike-in test with four standard strains – *E. coli* ATCC 25922, *S. aureus* ATCC 29213, *P. aeruginosa* ATCC 27853, and *E. faecalis* ATCC 29212 – and compared the QC range from CLSI to establish a threshold value. Based on an inspection of all the images, we determined that 20% growth compared with the control well was considered ‘growth’. However, for several combinations of bacteria and antimicrobials, the threshold values were adjusted because the growth rate over six hours of incubation was relatively slow or fast. For example, for tetracycline with *S. aureus* ATCC 29213, the growth rate was decelerated due to the antimicrobial effect; therefore, the threshold value was reduced to allow agreement with the BMD result. (Table 2.5 and Figure 2.21)

Threshold values of <i>E. coli</i> ATCC 25922 for Enterobacteriaceae sp p. and other Gram-negative species		Threshold values of <i>P. aeruginosa</i> ATCC 27853 for <i>P. aeruginosa</i>	
Antimicrobial	Threshold value	Antimicrobial	Threshold value
Ciprofloxacin	0.42	Imipenem	0.26
Amikacin	0.355	Cefotaxime	0.26
Imipenem	0.5	Fosfomycin	0.29
Meropenem	0.37	Ticarcillin/ clavulanic acid	0.43
		Aztreonam	0.6
		Piperacillin	0.26
		Ciprofloxacin	0.34
		Gentamicin	0.35
		Ticarcillin	0.67
Threshold values of <i>S. aureus</i> ATCC 29213 for <i>Staphylococcus</i> spp.		Threshold values of <i>E. faecalis</i> ATCC 29212 for <i>Enterococcus</i> spp.	
Antimicrobial	Threshold value	Antimicrobial	Threshold value
Ampicillin	0.15	Gentamicin	0.09
Oxacillin	0.32	Tetracycline	0.13
Tetracycline	0.113		
Levofloxacin	0.13		
Clindamycin	0.14		
Imipenem	0.29		

Table 2.5 Optimized threshold values. The general threshold value to determine the MIC was 0.2. The threshold values were optimized in the following cases. (Reprinted from [11])

**a**



**b**

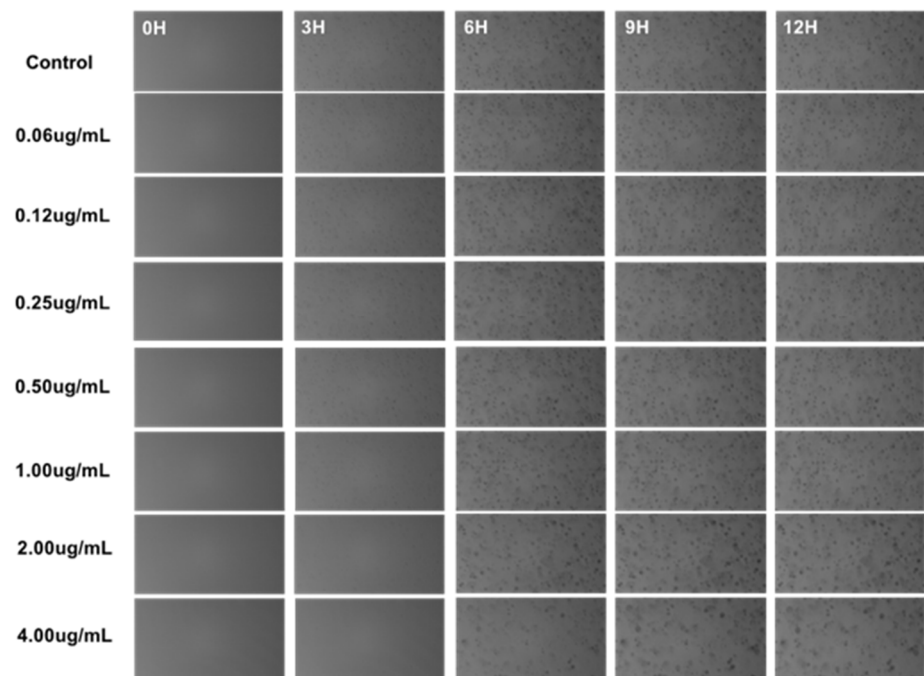


Figure 2.21 Time-lapse detection of decelerated growth rate due to antimicrobial effect (A) Time-lapse detection of *S.aureus* to the antibiotic erythromycin. (B) Time-lapse detection of *E.faecalis* to the antibiotic erythromycin. (Reprinted from [11])

Using this method, four standard strains were tested with clinically important antimicrobials in the DRAST chip, and the MIC values were calculated. To verify that the MIC values from DRAST were consistent with those from the gold standard method, the BMD test was performed simultaneously. In most cases, the MIC values were consistent with the values from BMD. (Table 2.6) In an example case, the normalized growth rate was greater than 20% until 16/8  $\mu\text{g/ml}$  and lower than 20% at 32/16  $\mu\text{g/ml}$ , implying a MIC of 32/16  $\mu\text{g/ml}$ . (Figure 2.20B) For the final determination of antimicrobial susceptibility, bacterial identification (ID) information is needed because MIC value must be interpreted using MIC interpretive standards, which vary with bacterial species. Next, antibiotic susceptibility was determined in a full antimicrobial panel. (Figure 2.20C)

Antimicrobial	MIC, DRAST (µg/ml)	MIC, BMD (µg/ml)	CLSI QC range (µg/ml)	MIC, DRAST (µg/ml)	MIC, BMD (µg/ml)	CLSI QC range (µg/ml)
(A) Gram-negative strains						
E. coli ATCC 25922			P. aeruginosa ATCC 27853			
Amikacin	2,4	2,4	0,5-4	2	1-4	1-4
Amoxicillin/ clavulanic acid	8/4	8/4	2/1-8/4	-	-	-
Aztreonam	0,25	0,12-0,5	0,06-0,25	4	2,4	2-8
Cefepime	0,06, 0,12	0,03, 0,12	0,015-0,12	2	1,2	0,5-4
Cefotaxime	-	-	-	32	16	8-32
Ceftazidime	-	-	-	2,4	2	1-4
Ciprofloxacin	-	-	-	0,25,0,5	0,25,0,5	0,25-1
Colistin	2	0,5,1	0,25-2	2,4	1	0,5-4
Fosfomycin	-	-	-	2,4	8	2-8
Gentamicin	1	0,25-1	0,25-1	1,2	1,2	0,5-2
Imipenem	-	-	-	2,4	4	1-4
Meropenem	-	-	-	0,5,1	0,5	0,25-1
Piperacillin	4	4	1-4	4,8	4	1-8
Piperacillin/ tazobactam	4/4	2/4,4/4	1/4-4/4	8/4	8/4	1/4-8/4
Trimethoprim/ sulfamethoxazole	≤0,5/9,5	≤0,5/9,5	≤0,5/9,5	-	-	-
Ticarcillin	16	8,16	4-16	16,32	16,32	8-32
Ticarcillin/ clavulanic acid	4/2	8/2, 16/2	4/2-16/2	-	-	-
Tobramycin	1	0,5,1	0,25-1	0,5,1	0,25,0,5	0,25-1
(B) Gram-positive strains						
S. aureus ATCC 29213			E. faecalis ATCC 29212			
Ampicillin	1	1,2	0,5-2	2	2	0,5-2
Ciprofloxacin	0,12,0,25	0,25,0,5	0,12-0,5	2	2	0,25-2
Clindamycin	0,12,0,25	0,12, 0,25	0,06-0,25	8,16	8, 16	4-16
Erythromycin	0,25, 0,5	0,5	0,25-1	2	1, 2	1-4
Gentamicin	0,5	0,25, 0,5	0,12-1	4	8	4-16
Imipenem	-	-	-	1,2	2	0,5-2
Levofloxacin	0,25	0,25	0,06-0,5	0,5	0,5, 1	0,25-2
Linezolid	1	4	1-4	1,2	2	1-4
Oxacillin	0,5	0,25, 0,5	0,12-0,5	16	8,16	8-32
Penicillin	0,5	0,5,1	0,25-2	2	2	1-4
Rifampin	-	-	-	1	1,2	0,5-4
Tetracycline	0,25,0,5	0,5,1	0,12-1	8	16,32	8-32

Table 2.6 MIC values from DRAST with spiked sample, broth microdilution test and CLSI quality control ranges. The DRAST test was performed on a positive blood culture sample spiked with four standard strains. The broth microdilution test was performed on a colony cultured on an LB agar plate. (Reprinted from [11])

## **Chapter 3.**

# **Platform validation: DRAST system with MALDI-TOF MS**

In this chapter, the workflow of direct identification of bacteria by MALDI-TOF MS and clinical validation results of DRAST system will be described. As MALDI-TOF MS was utilized as companion microbial identification technology of DRAST system, brief experimental procedures will be introduced. After that, the accuracy and discrepancy results of clinical study of DRAST system with MALDI-TOF MS will be described in detail based on bacterial species, kind of bacterial species and antimicrobials tested. In addition to the accuracy and discrepancy of DRAST system, the total turnaround time of DRAST system, which is one of the most important features will be covered with comparative results from conventional AST systems utilized in clinical settings. The final part of this chapter discusses about the subsequent clinical study of DRAST system against Gram-positive bacterial species for further validation.

### **3.1. Direct identification of bacteria from positive blood culture bottles**

#### **3.1.1. The workflow of direct identification of bacteria from positive blood culture bottles**

Performing the direct identification from positive blood cultures using MALDI-TOF MS can differ greatly but usually follow a similar workflow. (Figure 3.1) A sample of blood culture is drawn from the culture bottle and is centrifuged to pellet the red blood cells. High-speed centrifugation is performed to pellet the remaining pathogens. This pellet can be washed and centrifuged a few more times to increase the purity of bacterial pellets. Once purified, either an extraction can be performed or the bacteria can be added to a target plate and tested on a MALDI system for identification [44].

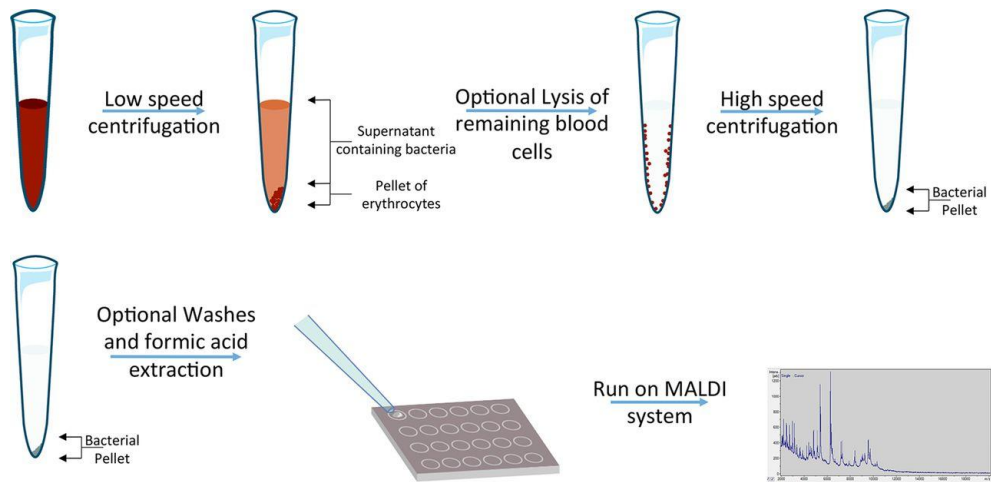


Figure 3.1 Procedures between studies to perform identification directly from positive blood cultures (Reprinted from [44])

### 3.1.2. Our workflow of direct identification of bacteria from positive blood culture bottles

A sample from a PBCB, the BACTEC Plus Aerobic/F, Lytic/10 and Anaerobic/F (Becton Dickinson Company, NJ, United States) or BacT/ALERT FA Plus and SN (BioMerieux Inc., Marcy l'Étoile, France), was processed using the Sepsityper kit (Billerica, MA, United States) before the analysis using the Bruker MALDI-TOF Biotyper system. Briefly, 1.0 ml of sample from a PBCB was transferred to a 1.5 ml centrifuge tube. A 200 µl aliquot of lysis buffer (provided) was added to the blood specimen, and the mixture was vortexed for 10 s prior to centrifugation (13,000 rpm, 2 min). Following centrifugation, the supernatant was removed, and the bacterial pellet was resuspended in 1.0 ml of wash buffer (provided), vortexed, and centrifuged (13,000 rpm, 1 min). The supernatant was

discarded, and the pellet was resuspended in 300  $\mu$ l of deionized water. Then, 900  $\mu$ l of 100% ethanol was added, and the mixture was vortexed and centrifuged at 13,000 rpm for 1 min. The ethanol was discarded, and the sample was again centrifuged at 13,000 rpm for 1 min. The pellet was allowed to dry completely. When dry, 70% formic acid (Sigma-Aldrich, MO, United States) at the same volume as the pellet ( $\sim$ 10  $\mu$ l) was added and mixed. The same volume ( $\sim$ 10  $\mu$ l) of acetonitrile (Sigma-Aldrich, MO, United States) was added, and the pellet went resuspension. The suspension was centrifuged a final time (13,000 rpm, 1 min), and 1  $\mu$ l of the resulting supernatant was analyzed using MALDI-TOF MS.

## **3.2. Clinical Study of DRAST with MALDI-TOF MS**

### **3.2.1. The accuracy and discrepancy results of clinical study of DRAST with MALDI-TOF MS**

We tested 105 Gram-negative and 101 Gram-positive strains from positive blood cultures. (Table 3.1 and Table 3.2) After the DRAST test, the positive blood culture sample was inoculated onto an LB agar plate for subculture, and the CFU was measured. The bacterial concentration ranged from  $1.3 \times 10^8$  to  $7.6 \times 10^9$  CFU/ml in Gram-negative strains and  $1.6 \times 10^7$  to  $7.6 \times 10^9$  CFU/ml in Gram-positive strains. (Figure 3.2) Using the colony on agar plate, we performed the BMD test as a reference test to validate the performance of the DRAST system. The image processing program automatically derived the AST results from the

DRAST images. The error rates were calculated by comparing the results from the DRAST system and BMD. (Table 3.3)

Bacteria identification			
Gram-negative	number	Gram-positive	number
<i>Escherichia coli</i>	50	<i>Staphylococcus aureus</i>	37
<i>Klebsiella pneumoniae</i>	23	<i>Enterococcus faecium</i>	23
<i>Pseudomonas aeruginosa</i>	9	<i>Staphylococcus epidermidis</i>	17
<i>Acinetobacter baumannii</i>	4	<i>Enterococcus faecalis</i>	12
<i>Citrobacter freundii</i>	4	<i>Staphylococcus haemolyticus</i>	8
<i>Proteus mirabilis</i>	2	<i>Staphylococcus hominis</i>	3
<i>Serratia marcescens</i>	2	<i>Staphylococcus caprae</i>	1
<i>Enterobacter aerogenes</i>	2	Sum	101
<i>Burkholderia cenocepacia</i>	2		
<i>Enterobacter asburiae</i>	1		
<i>Aeromonas veronii</i>	1		
<i>Klebsiella oxytoca</i>	1		
<i>Enterobacter hormaechei</i>	1		
<i>Acinetobacter nosocomialis</i>	1		
<i>Acinetobacter pittii</i>	1		
<i>Citrobacter braakii</i>	1		
Sum	105		

Table 3.1 Bacterial ID of 206 clinically isolated strains. There were 16 species of 105 Gram-negative strains and 7 species of 101 Gram-positive strains. (Reprinted from [11])

Classification for MIC interpretive standards	
Gram-negative	number
<i>Enterobacteriaceae</i> spp.	87
<i>Pseudomonas aeruginosa</i>	9
<i>Acinetobacter</i> spp.	6
Non- <i>Enterobacteriaceae</i>	1
<i>Burkholderia cenocepacia</i>	2
Gram-positive	number
<i>Staphylococcus</i> spp.	66
<i>Enterococcus</i> spp.	35

Table 3.2 Classification of clinical samples for MIC interpretive standards. (Reprinted from [11])

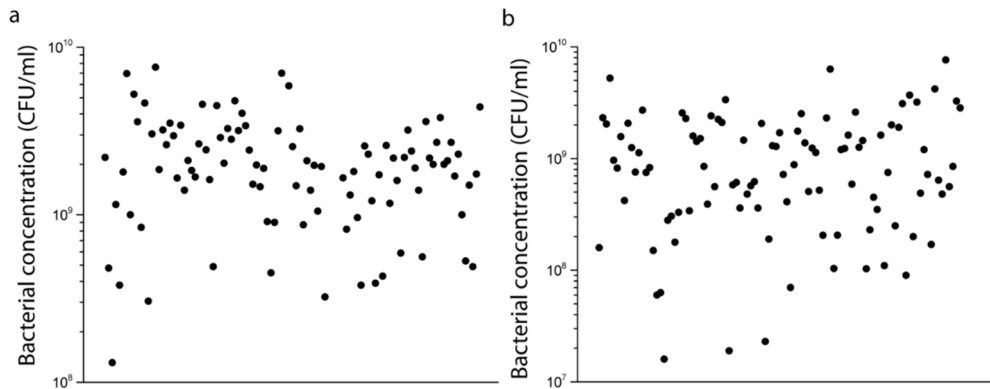


Figure 3.2 Number of bacteria in clinical PBCB samples. (a) Gram-negative strain bottle. The highest concentration was approximately  $7.6 \times 10^9$  CFU/ml, and the lowest was approximately  $1.3 \times 10^8$  CFU/ml. (b) Gram-positive strain bottle. The highest concentration was approximately  $7.6 \times 10^9$  CFU/ml, and the lowest was approximately  $1.6 \times 10^7$  CFU/ml. (Reprinted from [11])

Bacteria	n tests	BMD			Discrepancy number			Discrepancy rate (%)			
		S	I	R	mE	ME	VME	mE	ME	VME	CA
Gram-negative	1731	1178	114	439	140	29	5	8.09	2.46	1.14	89.95
Gram-positive	1137	659	21	457	52	21	8	4.57	3.19	1.75	92.88
Total	2868	1837	135	896	192	50	13	6.69	2.72	1.45	91.11

Table 3.3 Discrepancy rates and CA rates for DRAST using clinical samples. The DRAST results were compared with the BMD results to calculate the discrepancy rates. For the BMD test: S, susceptible; I, intermediate; R, resistant. For DRAST: mE, minor error; ME, major error; VME, very major error; CA, categorical agreement.

After 6 hours of incubation and image analysis, there was 11.6% of non-reliable growth in the sample that the image processing could not detect the substantial growth for determination of AST. 16 species of Gram-negative bacteria and seven species of Gram-positive bacteria were tested. Among the Gram-negative strains, 87 strains were classified as *Enterobacteriaceae* spp., and the others included nine *Pseudomonas aeruginosa* strains, six *Acinetobacter* spp. strains and three other species. Among the Gram-positive strains, 66 strains were classified as *Staphylococcus* spp., and 35 were classified as *Enterococcus* spp. These strains included strains of clinically important species, such as *Enterococcus faecium*, *Staphylococcus aureus*, *Klebsiella pneumoniae*, *Acinetobacter baumannii*, *Pseudomonas aeruginosa* and *Enterobacter* spp. (ESKAPE) strains. A total of 1731 tests were performed using Gram-negative strains, and there were 140 minor errors (mEs), 29 major errors (MEs) and 5 very major errors (VMEs). (Table 3.4)

Antimicrobial	n tests	BMD			Discrepancy number			Discrepancy rate (%)			
		S	I	R	mE	ME	VME	mE	ME	VME	CA
Amoxicillin/clavulanic acid	90	52	18	20	18	1	0	20.00%	1.92%	0.00%	78.89%
Amikacin	105	98	0	7	0	0	0	0.00%	0.00%	0.00%	100.00%
Aztreonam	99	64	7	28	6	6	0	6.06%	9.38%	0.00%	87.88%
Cefepime	105	71	5	29	11	1	0	10.48%	1.41%	0.00%	88.57%
Cefotaxime	96	59	2	35	2	5	0	2.08%	8.47%	0.00%	92.71%
Ceftazidime	105	70	2	33	10	2	0	9.52%	2.86%	0.00%	88.57%
Ciprofloxacin	105	63	5	37	5	0	0	4.76%	0.00%	0.00%	95.24%
Colistin	15	13	1	1	3	0	1	20.00%	0.00%	100.00%	73.33%
Fosfomycin	87	49	11	27	19	0	1	21.84%	0.00%	3.70%	77.01%
Gentamicin	105	81	0	24	0	0	0	0.00%	0.00%	0.00%	100.00%
Imipenem	105	86	5	14	8	0	0	7.62%	0.00%	0.00%	92.38%
Meropenem	105	92	1	12	1	0	0	0.95%	0.00%	0.00%	99.05%
Piperacillin/tazobactam	105	88	2	15	6	4	0	5.71%	4.55%	0.00%	90.48%
Piperacillin	102	52	4	46	17	2	2	16.67%	3.85%	4.35%	79.41%
Ticarcillin/clavulanic acid	102	51	23	28	17	0	0	16.67%	0.00%	0.00%	83.33%
Trimethoprim/Sulfamethoxazole	96	70	0	26	0	7	0	0.00%	10.00%	0.00%	92.71%
Ticarcillin	102	41	22	39	11	0	0	10.78%	0.00%	0.00%	89.22%
Tobramycin	102	78	6	18	6	1	1	5.88%	1.28%	5.56%	92.16%
Total	1731	1178	114	439	140	29	5	8.09%	2.46%	1.14%	89.95%

Table 3.4 Summary of clinical testing of Gram-negative strains using DRAST, according to the antimicrobial applied. (Reprinted from [11])

For determination of discrepancies, discrepancies are classified as follows according to FDA guidance. mE stands for which reference results is resistant or susceptible and device results is intermediate; reference result is intermediate and device result is resistant or susceptible. ME stands for which reference result is susceptible and device result is resistant. VME represents for which reference results is resistant and device result is susceptible. FDA guidelines Among the 29 MEs, seven MEs occurred in trimethoprim/sulfamethoxazole (T/S). The 5 VMEs occurred in one in colistin, fosfomycin and tobramycin and two in piperacillin. The VMEs in Gram-negative strains included four from *Enterobacteriaceae* spp. with

fosfomycin, piperacillin and tobramycin as well as one from *Acinetobacter* spp. with colistin. (Table 3.5 – Table 3.7) For the Gram-positive strains, 1137 tests were conducted, and there were 52 mEs, 21 MEs and 8 VMEs. (Table 3.8)

Antimicrobial	n tests	BMD			Discrepancy number			Discrepancy rate (%)			
		S	I	R	mE	ME	VME	mE	ME	VME	CA
Amoxicillin/clavulanic acid	87	50	18	19	17	1	0	19.54%	2.00%	0.00%	79.31%
Amikacin	87	84	0	3	0	0	0	0.00%	0.00%	0.00%	100.00%
Aztreonam	87	59	3	25	3	6	0	3.45%	10.17%	0.00%	89.66%
Cefepime	87	62	3	22	10	1	0	11.49%	1.61%	0.00%	87.36%
Cefotaxime	87	56	1	30	1	5	0	1.15%	8.93%	0.00%	93.10%
Ceftazidime	87	61	2	24	9	2	0	10.34%	3.28%	0.00%	87.36%
Ciprofloxacin	87	54	4	29	4	0	0	4.60%	0.00%	0.00%	95.40%
Colistin	-	-	-	-	-	-	-	-	-	-	-
Fosfomycin	87	49	11	27	19	0	1	21.84%	0.00%	3.70%	77.01%
Gentamicin	87	69	0	18	0	0	0	0.00%	0.00%	0.00%	100.00%
Imipenem	87	80	3	4	6	0	0	6.90%	0.00%	0.00%	93.10%
Meropenem	87	85	0	2	0	0	0	0.00%	0.00%	0.00%	100.00%
Piperacillin/tazobactam	87	79	1	7	5	4	0	5.75%	5.06%	0.00%	89.66%
Piperacillin	87	46	4	37	15	2	2	17.24%	4.35%	5.41%	78.16%
Ticarcillin/clavulanic acid	87	49	19	19	14	0	0	16.09%	0.00%	0.00%	83.91%
Trimethoprim/ Sulfamethoxazole	87	66	0	21	0	6	0	0.00%	9.09%	0.00%	93.10%
Ticarcillin	87	40	17	30	8	0	0	9.20%	0.00%	0.00%	90.80%
Tobramycin	87	69	6	12	6	1	1	6.90%	1.45%	8.33%	90.80%
Total	1479	1058	92	329	117	28	4	7.91%	2.65%	1.22%	89.93%

Table 3.5 Summary of clinical testing of Enterobacteriaceae spp. strains using DRAST, according to the applied the antimicrobial applied. (Reprinted from [11])

Antimicrobial	n tests	BMD			Discrepancy number			Discrepancy rate (%)			
		S	I	R	mE	ME	VME	mE	ME	VME	CA
Amoxicillin/clavulanic acid	-	-	-	-	-	-	-	-	-	-	-
Amikacin	9	9	0	0	0	0	0	0.00%	0.00%	nan%	100.00%
Aztreonam	9	2	4	3	2	0	0	22.22%	0.00%	0.00%	77.78%
Cefepime	9	5	2	2	1	0	0	11.11%	0.00%	0.00%	88.89%
Cefotaxime	-	-	-	-	-	-	-	-	-	-	-
Ceftazidime	9	5	0	4	0	0	0	0.00%	0.00%	0.00%	100.00%
Ciprofloxacin	9	6	0	3	0	0	0	0.00%	0.00%	0.00%	100.00%
Colistin	9	8	1	0	3	0	0	33.33%	0.00%	nan%	66.67%
Fosfomycin	-	-	-	-	-	-	-	-	-	-	-
Gentamicin	9	7	0	2	0	0	0	0.00%	0.00%	0.00%	100.00%
Imipenem	9	2	2	5	2	0	0	22.22%	0.00%	0.00%	77.78%
Meropenem	9	3	1	5	1	0	0	11.11%	0.00%	0.00%	88.89%
Piperacillin/tazobactam	9	5	1	3	0	0	0	0.00%	0.00%	0.00%	100.00%
Piperacillin	9	5	0	4	1	0	0	11.11%	0.00%	0.00%	88.89%
Ticarcillin/clavulanic acid	9	1	4	4	2	0	0	22.22%	0.00%	0.00%	77.78%
Trimethoprim/ Sulfamethoxazole	-	-	-	-	-	-	-	-	-	-	-
Ticarcillin	9	0	5	4	2	0	0	22.22%	-	0.00%	77.78%
Tobramycin	9	7	0	2	0	0	0	0.00%	0.00%	0.00%	100.00%
Total	126	65	20	41	14	0	0	11.11%	0.00%	0.00%	88.89%

Table 3.6 Summary of clinical testing of *Pseudomonas aeruginosa* strains using DRAST, according to the antimicrobial applied. (Reprinted from [11])

Antimicrobial	n tests	BMD			Discrepancy number			Discrepancy rate (%)				
		S	I	R	mE	ME	VME	mE	ME	VME	CA	
Amoxicillin/clavulanic acid	-	-	-	-	-	-	-	-	-	-	-	-
Amikacin	6	2	0	4	0	0	0	0.00%	0.00%	0.00%	100.00%	
Aztreonam	-	-	-	-	-	-	-	-	-	-	-	-
Cefepime	6	1	0	5	0	0	0	0.00%	0.00%	0.00%	100.00%	
Cefotaxime	6	0	1	5	1	0	0	16.67%	-	0.00%	83.33%	
Ceftazidime	6	1	0	5	1	0	0	16.67%	0.00%	0.00%	83.33%	
Ciprofloxacin	6	1	0	5	0	0	0	0.00%	0.00%	0.00%	100.00%	
Colistin	6	5	0	1	0	0	1	0.00%	0.00%	100.00%	83.33%	
Fosfomycin	-	-	-	-	-	-	-	-	-	-	-	-
Gentamicin	6	2	0	4	0	0	0	0.00%	0.00%	0.00%	100.00%	
Imipenem	6	1	0	5	0	0	0	0.00%	0.00%	0.00%	100.00%	
Meropenem	6	1	0	5	0	0	0	0.00%	0.00%	0.00%	100.00%	
Piperacillin/tazobactam	6	1	0	5	1	0	0	16.67%	0.00%	0.00%	83.33%	
Piperacillin	6	1	0	5	1	0	0	16.67%	0.00%	0.00%	83.33%	
Ticarcillin/clavulanic acid	6	1	0	5	1	0	0	16.67%	0.00%	0.00%	83.33%	
Trimethoprim/ Sulfamethoxazole	6	1	0	5	0	1	0	0.00%	100.00%	0.00%	83.33%	
Ticarcillin	6	1	0	5	1	0	0	16.67%	0.00%	0.00%	83.33%	
Tobramycin	6	2	0	4	0	0	0	0.00%	0.00%	0.00%	100.00%	
Total	90	21	1	68	6	1	1	6.67%	4.76%	1.47%	91.11%	

Table 3.7 Summary of clinical testing of *Acinetobacter* spp. strains using DRAST, according to the antimicrobial applied. (Reprinted from [11])

Antimicrobial	n tests	BMD			Discrepancy number			Discrepancy rate			
		S	I	R	mE	ME	VME	mE	ME	VME	CA
Ampicillin	35	13	0	22	0	0	0	0.00%	0.00%	0.00%	100.00%
Ciprofloxacin	101	37	0	64	6	0	0	5.94%	0.00%	0.00%	94.06%
Clindamycin	66	51	1	14	1	0	0	1.52%	0.00%	0.00%	98.48%
Erythromycin	101	34	6	61	18	1	1	17.82%	2.94%	1.64%	80.20%
Gentamicin	66	37	6	23	5	0	0	7.58%	0.00%	0.00%	92.42%
Imipenem	66	41	0	25	0	4	1	0.00%	9.76%	4.00%	92.42%
Levofloxacin	101	37	0	64	3	0	0	2.97%	0.00%	0.00%	97.03%
Linezolid	101	100	1	0	2	2	0	1.98%	2.00%	nan%	96.04%
Oxacillin	65	28	0	37	0	0	1	0.00%	0.00%	2.70%	98.46%
Penicillin	101	14	0	87	0	1	3	0.00%	7.14%	3.45%	96.04%
Rifampin	66	52	2	12	2	1	0	3.03%	1.92%	0.00%	95.45%
Trimethoprim/ Sulfamethoxazole	66	52	0	14	0	11	1	0.00%	21.15%	7.14%	81.82%
Tetracycline	101	81	1	19	7	1	0	6.93%	1.23%	0.00%	92.08%
Vancomycin	101	82	4	15	8	0	1	7.92%	0.00%	6.67%	91.09%
Total	1137	659	21	457	52	21	8	4.57%	3.19%	1.75%	92.88%

Table 3.8 Summary of clinical testing of Gram-positive strains using DRAST,

according to the antimicrobial applied. (Reprinted from [11])

Among the nine VMEs in Gram-positive strains, three VMEs were from penicillin and one was from oxacillin, erythromycin, imipenem and T/S in *Staphylococcus* spp. (Table 3.9 and Table 3.10)

Antimicrobial	n tests	BMD			Discrepancy number			Discrepancy rate (%)			
		S	I	R	mE	ME	VME	mE	ME	VME	CA
Ampicillin	-	-	-	-	-	-	-	-	-	-	-
Ciprofloxacin	66	33	0	33	4	0	0	6.06%	0.00%	0.00%	93.94%
Clindamycin	66	51	1	14	1	0	0	1.52%	0.00%	0.00%	98.48%
Erythromycin	66	30	4	32	13	1	1	19.70%	3.33%	3.12%	77.27%
Gentamicin	66	37	6	23	5	0	0	7.58%	0.00%	0.00%	92.42%
Imipenem	66	41	0	25	0	4	1	0.00%	9.76%	4.00%	92.42%
Levofloxacin	66	33	0	33	2	0	0	3.03%	0.00%	0.00%	96.97%
Linezolid	66	66	0	0	0	2	0	0.00%	3.03%	-	96.97%
Oxacillin	65	28	0	37	0	0	1	0.00%	0.00%	2.70%	98.46%
Penicillin	66	4	0	62	0	1	3	0.00%	25.00%	4.84%	93.94%
Rifampin	66	52	2	12	2	1	0	3.03%	1.92%	0.00%	95.45%
Trimethoprim/ Sulfamethoxazole	66	52	0	14	0	11	1	0.00%	21.15%	7.14%	81.82%
Tetracycline	66	57	1	8	7	1	0	10.61%	1.75%	0.00%	87.88%
Vancomycin	66	62	4	0	6	0	0	9.09%	0.00%	-	90.91%
Total	857	546	18	293	40	21	7	4.67%	3.85%	2.39%	92.07%

Table 3.9 Summary of clinical testing of *Staphylococcus* spp. strains using DRAST according to the applied antimicrobial applied.

Antimicrobial	n tests	BMD			Discrepancy number			Discrepancy rate (%)			
		S	I	R	mE	ME	VME	mE	ME	VME	CA
Ampicillin	35	13	0	22	0	0	0	0.00%	0.00%	0.00%	100.00%
Ciprofloxacin	35	4	0	31	2	0	0	5.71%	0.00%	0.00%	94.29%
Clindamycin	-	-	-	-	-	-	-	-	-	-	-
Erythromycin	35	4	2	29	5	0	0	14.29%	0.00%	0.00%	85.71%
Gentamicin	-	-	-	-	-	-	-	-	-	-	-
Imipenem	-	-	-	-	-	-	-	-	-	-	-
Levofloxacin	35	4	0	31	1	0	0	2.86%	0.00%	0.00%	97.14%
Linezolid	35	34	1	0	2	0	0	5.71%	0.00%	nan%	94.29%
Oxacillin	-	-	-	-	-	-	-	-	-	-	-
Penicillin	35	10	0	25	0	0	0	0.00%	0.00%	0.00%	100.00%
Rifampin	-	-	-	-	-	-	-	-	-	-	-
Trimethoprim/ Sulfamethoxazole	-	-	-	-	-	-	-	-	-	-	-
Tetracycline	35	24	0	11	0	0	0	0.00%	0.00%	0.00%	100.00%
Vancomycin	35	20	0	15	2	0	1	5.71%	0.00%	6.67%	91.43%
Total	280	113	3	164	12	0	1	4.29%	0.00%	0.61%	95.36%

Table 3.10 Summary of clinical testing of *Enterococcus* spp. strains using DRAST according to the antimicrobial applied.

There were 11 MEs in T/S with Gram-positive strains. In T/S, small microcolonies were observed even in susceptible cases, and the difference between susceptible and resistant was not clear. In some cases, the microcolonies in the processed images were out of focus and were not detected. (Figure 3.3) In cases in which the number of microcolonies was smaller than the number in the control, the area was not 20% larger than the control, and the sample was regarded as susceptible, i.e., possibly resistant in the BMD test. The categorical agreement rates for the DRAST clinical samples according to the main classified strains were 89.9% in *Enterobacteriaceae* spp., 88.9% in *P. aeruginosa*, 92.1% in *Staphylococcus* spp. and 95.4% in *Enterococcus* spp. (Figure 3.4)

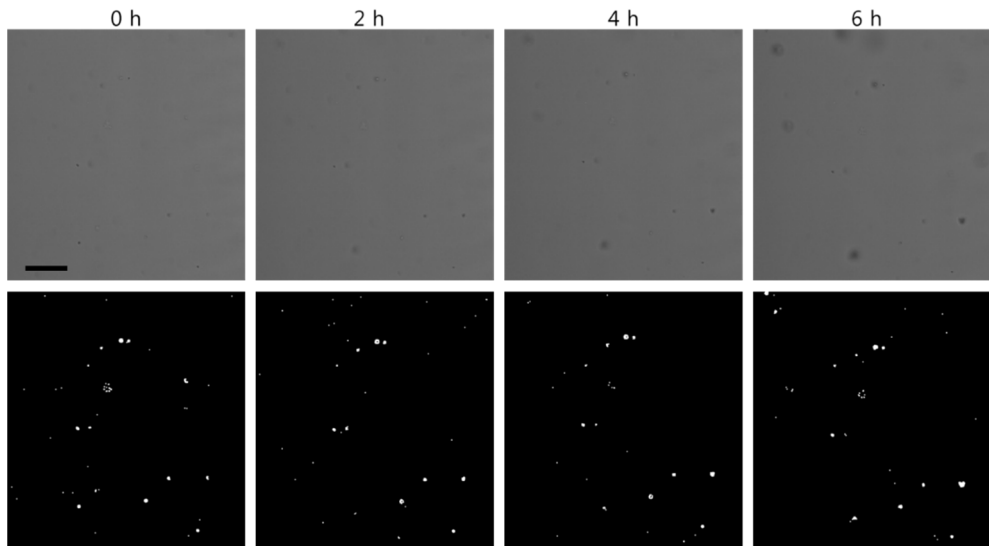


Figure 3.3 Time-lapse images of microcolonies of *Staphylococcus hominis* with trimethoprim/sulfamethoxazole. In the raw images, few microcolonies were visible. However, some of the microcolonies were out of focus and not detected in the processed images. The scale bar represents 300  $\mu\text{m}$ .

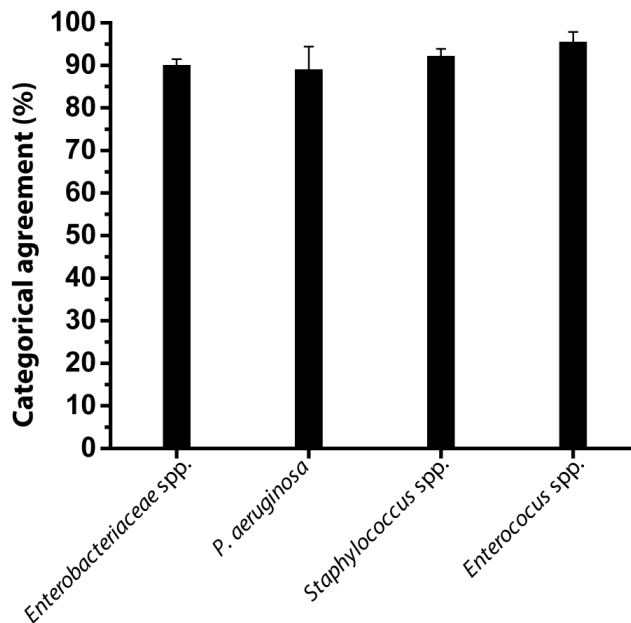


Figure 3.4 CA rates according to the main classified strains: *Enterobacteriaceae* spp. (n=87, 89.9%), *P. aeruginosa* (n=9, 88.9%), *Staphylococcus* spp. (n=66, 92.1%), *Enterococcus* spp. (n=35, 95.4%). Error bars represent 95% confidence intervals. (Reprinted from [11])

The discrepancy rates are shown in Figure 3.5. The total number of *P. aeruginosa* samples in the clinical testing was nine, and most of the mEs were due to filament formation induced by beta-lactam antibiotics. Some cases were classified as ‘growth’ because the low-magnification imaging system was not capable of differentiating between division and filament formation. The results showed a categorical agreement of 91.11%, minor error of 6.69%, major error of 2.72%, and very major error of 1.45%. According to the US FDA, for the acceptable performance of susceptibility tests, the overall categorical agreement

should be higher than 90%, with mEs  $\leq 10\%$ , MEs  $\leq 3\%$  and VMEs  $\leq 1.5\%$  [45]. Including all these reasons for error, the DRAST system satisfied the FDA's recommended performance guidelines.

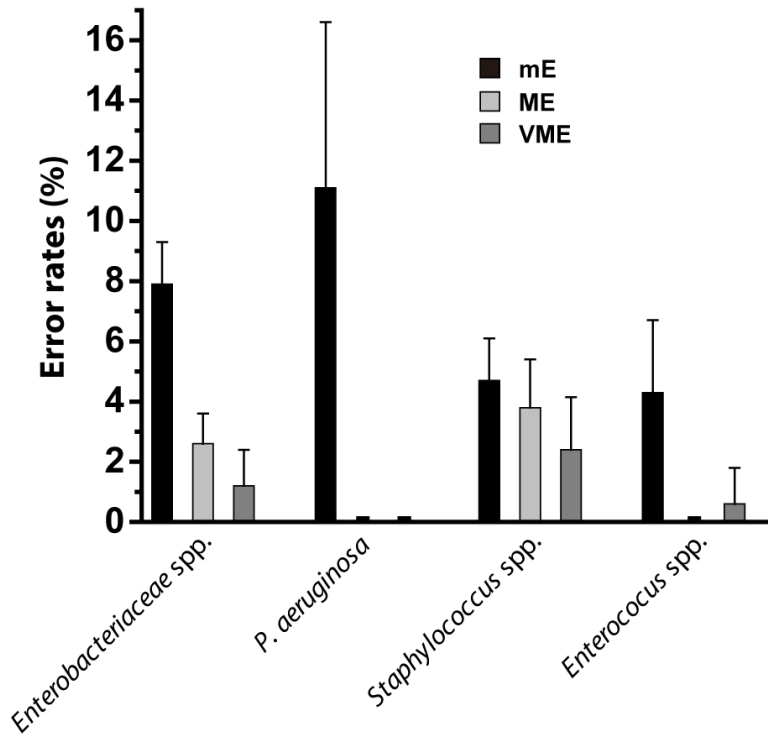


Figure 3.5 Discrepancy rates according to the main classified strains: Enterobacteriaceae spp. (mE=7.9%, ME=2.6%, VME=1.2%), *P. aeruginosa* (mE=11.1%, ME=0.0%, VME=0.0%), Staphylococcus spp. (mE=4.7%, ME=3.8%, VME=2.4%), and Enterococcus spp. (mE=4.3%, ME=0.0%, VME=0.6%). The error rates were calculated by comparing the AST results from each method with the BMD test. Error bars represent 95% confidence intervals. (Reprinted from [11])

### 3.2.2. The total turnaround results of clinical study of DRAST with MALDI-TOF MS

The time required for AST was compared using DRAST and the conventional method, Vitek 2 or MicroScan. (Figure 3.6) In the case of DRAST, the average turnaround time for AST from a PBCB was 15.1 hours which includes the delay time in average nine hours between positive signal of blood culture and initiation of DRAST. (Figure 3.6A) The time required for AST was only six hours; the remaining turnaround time was due to delayed tests flagged as positive. In the workflow of a clinical setting, flagged blood culture samples from overnight culture would be batch processed in the morning. The time required for AST using Vitek 2 and MicroScan, which include a subculture process, was 48.1 hours and 56.0 hours, respectively. The total time from blood collection was also compared. (Figure 3.6B) In both cases, DRAST saved approximately 36 hours compared to the conventional methods.

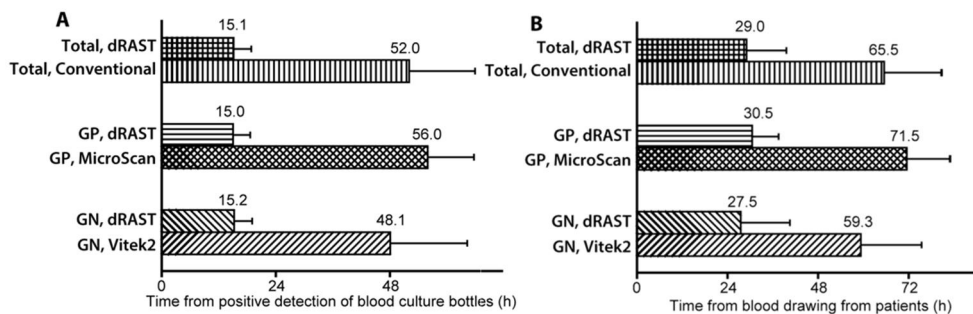


Figure 3.6 Average time to results of AST from (A) time of positive detection of blood culture bottles or (B) time of blood collection from patient. The time

required for AST using DRAST and a conventional AST method requiring subculture (Vitek 2 or MicroScan) was calculated. (Reprinted from [11])

### **3.3. Clinical Study of DRAST of Gram-positive clinical strains with MALDI-TOF MS**

For further validation of DRAST system in clinical settings, we did another clinical study with Gram-positive pathogens in SNUH. The sample collection and processing was identical with those of previous study. Total 115 positive blood culture samples of Gram-positive cocci were investigated and a complete list of tested organisms was presented. (Table 3.11) There were 76 *Staphylococcus* spp. including 42 *S. aureus*, 23 *S. epidermidis*, 8 *S. haemolyticus*, and 3 *S. hominis*. There were 39 *Enterococcus* spp. including 24 *E. faecium*, 14 *E. faecalis* and one *E. gallinarum*. These GPC isolates were used for interpreting MIC and interpretative AST results.

Genus	Species	No. (%)
<i>Staphylococcus</i> spp.	<i>Staphylococcus aureus</i>	42 (36.5)
	<i>Staphylococcus epidermidis</i>	23 (20.0)
	<i>Staphylococcus haemolyticus</i>	8 (7.0)
	<i>Staphylococcus hominis</i>	3 (2.6)
<i>Enterococcus</i> spp.	<i>Enterococcus faecium</i>	24 (20.9)
	<i>Enterococcus faecalis</i>	14 (12.2)
	<i>Enterococcus gallinarum</i>	1 (0.9)
Total		115 (100)

Table 3.11 Distribution of Gram-positive cocci from PBCs used in this study (Reprinted from [25])

### 3.3.1. The performance of DRAST system against Gram-positive cocci with MALDI-TOF MS

The AST results of the DRAST system for Gram-positive cocci from 115 (1,187 antimicrobial agent-microorganism combinations) PBCB samples are shown in the Table 2. For 115 Gram-positive samples, through the DRAST system, we observed 94.9% of CA and 98.3% of EA between DRAST system and MicroScan WalkAway plus system, respectively. The discrepancy rates DRAST were VME of 1.0% (5/485), ME of 1.2% (9/693) and mE of 4.0% (47/1,187), respectively. The highest CA was observed from ampicillin (100%), followed by linezolid (99.1%). Lowest CA was shown from erythromycin (84.3%) and ciprofloxacin (89.6%). The DRAST system yielded over 90% of CA for each antimicrobial except two antimicrobial agents; erythromycin and ciprofloxacin. The majority of discrepancies was classified as mEs.

(Abbreviations; CA, Category agreement; EA, Essential agreement; VME, Very major error; ME, Major error; mE, minor error)

Antimicrobial agents	No. of test	No. (%) of error			CA (%)	EA (%)
		VME	ME	mE		
Ampicillin	39	0	0	0	100	100
Ciprofloxacin	115	0	1 (2.4)	11 (9.6)	89.6	99.1
Clindamycin	76	0	0	1 (1.3)	98.7	100
Erythromycin	115	1 (1.4)	2 (5.3)	15 (13.0)	84.3	88.7
Gentamicin	73	1 (3.4)	0	5 (6.8)	91.8	100
Levofloxacin	115	0	0	4 (3.5)	96.5	97.5
Linezolid	115	0	0	1 (0.9)	99.1	100
Oxacillin	42	1 (5.6)	0	0	97.6	100
Penicillin	115	2 (2.0)	0	0	98.3	97.4
Rifampin	76	0	2 (3.1)	0	97.4	98.7
Trimethoprim/Sulfamethoxazole	76	0	4 (6.3)	0	94.7	98.7
Tetracycline	115	0	0	4 (3.5)	96.5	100
Vancomycin	115	0	0	6 (5.2)	94.8	99.1
Total	1,187	5 (1.0)	9 (1.2)	47 (4.0)	94.9	98.3

Table 3.12 Agreement rates in AST results between DRAST system and MicroScan WalkAway plus system for Gram-positive cocci (Reprinted from [25])

The discrepancy rates for to DRAST results compared to those from MicroScan WalkAway plus system in species level are shown in Table 3.13. The DRAST system yielded CA 96.8%, EA 97.8% in *S. aureus*, CA 90.9%, EA 98.7% in CNS and CA 96.5, EA 98.7% in Enterococcus spp., respectively. (Table 3.13)

Specifically, four VMEs and two MEs were observed from *S. aureus* in the DRAST system. Regarding the lowest CA from erythromycin-*S. aureus* combination, majority of discrepancies were determined as mEs. One of 18 oxacillin-resistant *S. aureus* and one of 15 erythromycin-resistant *S. aureus* were not determined as resistant by the DRAST system. From majority of antimicrobial agents except erythromycin, CA exceeded 95% in *S. aureus*. For CNS, only one

VME and seven MEs were observed in the DRAST results. Among the seven MEs, three MEs were detected from Trimethoprim/Sulfamethoxazole and mEs occurred mostly from ciprofloxacin, gentamicin, erythromycin, and vancomycin. For *Enterococcus* spp., no VME and ME were found, however, mE were mostly observed from erythromycin and vancomycin. All vancomycin-resistant *Enterococcus* were detected as resistant by the DRAST system. In overall, mE accounted for the most of errors from the tests with all antimicrobial agents. (Table 3.13) The DRAST results were available within 6 hours after inoculation into the DRAST GP panel, which were concordant with previous research [11].

Microorganism(s) and antimicrobial agents	No. of samples with susceptibility		No. (%) of errors			CA (%)	EA (%)
	S	R	VME	ME	mE		
<i>S. aureus</i> (n=42)							
Ciprofloxacin	29	13	0	0	2 (4.8)	95.2	100
Clindamycin	27	15	0	0	1 (2.4)	97.6	100
Erythromycin	27	15	1 (6.7)	1 (3.7)	6 (14.3)	81	83.3
Gentamicin	32	7	0	0	0	100	100
Levofloxacin	30	12	0	0	0	100	100
Linezolid	42	0	0	0	0	100	100
Oxacillin	24	18	1 (5.6)	0	0	97.6	92.9
Penicillin	1	41	2 (4.9)	0	0	95.2	92.9
Rifampin	41	1	0	0	0	100	100
Trimethoprim/Sulfamethoxazole	42	0	0	1 (2.4)	0	97.6	97.6
Tetracycline	35	7	0	0	1 (2.4)	97.6	100
Vancomycin	42	0	0	0	0	100	100
Total	372	129	4 (3.1)	2 (0.5)	10 (2.0)	96.8	97.8
<i>CNS</i> (n=34)							
Ciprofloxacin	8	26	0	1 (12.5)	7 (20.6)	76.5	97.1
Clindamycin	17	16	0	0	0	100	100
Erythromycin	9	25	0	1 (11.1)	4 (11.8)	85.3	91.2
Gentamicin	7	22	1 (4.5)	0	5 (15.2)	81.8	100
Levofloxacin	8	26	0	0	3 (8.8)	91.2	100
Linezolid	34	0	0	0	0	100	100
Penicillin	0	34	0	0	0	100	100
Rifampin	24	10	0	2 (8.3)	0	91.2	97.1
Trimethoprim/Sulfamethoxazole	21	13	0	3 (14.3)	0	91.2	100
Tetracycline	27	7	0	0	3 (8.8)	91.2	100
Vancomycin	34	0	0	0	4 (11.8)	88.2	100
Total	189	179	1 (0.6)	7 (3.7)	26 (7.0)	90.9	98.7
<i>Enterococcus</i> (n=39)							
Ampicillin	15	24	0	0	0	100	100
Ciprofloxacin	4	33	0	0	2 (5.1)	94.9	100
Erythromycin	4	34	0	0	5 (12.8)	87.2	92.3
Levofloxacin	6	33	0	0	1 (2.6)	97.4	100
Linezolid	39	0	0	0	1 (2.6)	97.4	100
Penicillin	14	25	0	0	0	100	100
Tetracycline	26	13	0	0	0	100	100
Vancomycin	24	15	0	0	2 (12.8)	94.9	97.4
Total	132	177	0	0	11 (4.5)	96.5	98.7

Table 3.13 Discrepancy rates and agreement rates of two AST systems in this clinical evaluation classified into combination of antimicrobial agents and bacterial species (Reprinted from [25])

### **3.3.2. Discussions of performance of DRAST system against Gram-positive cocci with MALDI-TOF MS**

This study focused on whether the DRAST system could be utilized routinely to reduce time for AST results of staphylococci and enterococci by comparing results between DRAST system from PBCBs and MicroScan WalkAway plus system. As a result, the DRAST system evaluated 1,187 antimicrobial Gram-positive cocci combinations, showing 94.9% overall CA and 98.3% overall EA, with only 1.0% VME and 1.3% ME. These results indicate that the antimicrobial agreement rate of DRAST from PBCBs with Gram-positive cocci was comparable or superior to that of other studies [46-48]. It is noteworthy that the detection of oxacillin-resistant staphylococci with the DRAST system was accurate even if one VME was observed in *S. aureus*, this result agreed with other standard AST reporting for oxacillin-resistance detection, for the agreement rates ranged from 95 to 100% [49, 50]. Also, the DRAST yielded high accuracy for the detection of vancomycin-resistant enterococci. Interestingly, no errors were observed for vancomycin and linezolid, the most frequently used antibiotics to treat systemic infections caused by staphylococci and enterococci. These results showed that DRAST system can precisely detect the antimicrobial resistance of medically significant Gram-positive cocci. However, there lie some limitations to this study. The DRAST panel did not cover some concentrations of oxacillin necessary for interpreting CNS. Further studies are necessary to confirm the reliability of this method with various kinds of pathogens with different resistance phenotypes.

## Chapter 4.

### Conclusion

In this dissertation, I proposed and developed direct, rapid antimicrobial susceptibility testing system with the utilization of biochip and time-lapse colony tracking methods which are critically needed by sepsis patients. The current AST diagnostics procedures, which is the test to determine the appropriate antimicrobial prescription, takes approximately three days from blood collection. To shorten this time, direct AST methods using PBCBs with no separation process, which was proposed and developed in this dissertation could be an attractive candidate. However, performing direct AST from PBCBs is technically difficult because the inoculum size cannot be effectively controlled, substances in the specimens such as antimicrobial absorption materials in blood cultures could affect the results, and the bottle could contain a polymicrobial culture containing more than two organisms [51]. To resolve this technical hurdles, I am preparing rapid purified microbial culture using ultrasensitive nanobeads which are able to capture pathogens from whole blood. With this rapid purified microbial culture with suitable microbial quantification methods integrated, it will be able to inoculate the same microbial loads into tests, inducing more controlled inoculum sizes in AST.

In conventional AST, which measures the optical density in a test well, the inoculum size must be controlled for consistent AST results. In the DRAST system proposed in this dissertation, the response of individual bacteria to antimicrobials was measured by observing microcolony formation from a single bacterium. Therefore, this method can generate consistent AST results with a wide range of inoculum sizes, from the typical bacterial concentrations in PBCBs. Additionally, the PBCB aliquot is diluted 4000-fold in the final test well, and additional substances in the blood culture specimens did not affect the AST result. Therefore, the accuracy of AST result from the DRAST system satisfied the FDA's recommendation. When they are flagged as positive for growth by the blood culture instrument, cultured bacteria from patients are mixed with hemocytes:  $\sim 10^9$  erythrocytes and  $\sim 10^6$  leukocytes per 1 ml of blood. The conventional AST systems Vitek 2 and MicroScan are not capable of differentiating the change in optical density (OD) of culture media mixed with hemocytes. Therefore, these systems require a subculture process involving an additional 1 day of incubation. In this dissertation, I developed the DRAST system using PBCBs without subculture process. Our group previously introduced a rapid AST method of imaging bacteria immobilized in an agarose gel matrix [20, 33, 52].

As mentioned above, polymicrobial infection is a fundamental barrier to direct AST. Approximately 5%~10% of BSI cases occur to be polymicrobial infections, and their mortality is higher than for monomicrobial infections [53, 54]. The current MALDI-TOF MS technology cannot identify multiple organisms in

polymicrobial cultures [55]. A trial was conducted to evaluate the identification of polymicrobial using differences between the MS fingerprints of bacteria [56]. At the time DRAST system was evaluated in clinical settings, as it was not fully automated, imaging times were set to 0, 2, 4 and 6 hours after incubation and imaging after 6 hours for the non-reliable growth cases after examining the growth condition was not feasible due to the technical limitation. This issue is now resolved by the realization of full automated system which control multiple DRAST chips and real time image processing to determine the AST results. Also, as there is some possibilities of different growth pattern after 6 hours of incubation in certain bacterial strains, the broad database on growth pattern according to the bacterial ID could contribute to predict the case and reduce the error.

In this dissertation, by eliminating the subculture process, the DRAST system could perform AST in six hours through microcolony detection under a microscope. Consequently, the DRAST system reduced the time from a positive signal from blood culture until AST from 40 hours to six hours. Assuming practical utilization in laboratory medicine, it would be possible to shorten the time required to obtain results by two days. The average time to detect a positive blood culture is approximately 16 hours [57]. Therefore, the total time from blood collection to the AST result was 24 hours using the DRAST system. Additionally, the DRAST system satisfied the performance recommendations of the US FDA. According to a literature survey, the time reduction in AST could decrease mortality and hospitalization periods [58-61]. The DRAST system could increase the survival

rate of sepsis patients. For the accurate prescription of antimicrobials to patients, ID information of bacterial pathogen is a prerequisite for interpreting the MIC results from AST because the MIC interpretation criteria vary according to the species of bacteria [62]. The bacterial identification result should be acquired prior to the AST result. As, the MALDI-TOF MS system was validated for direct ID of bacterial species from positive blood cultures in one hour, including preparation time [55, 63]. Combining the DRAST system with direct ID using a MALDI Biotyper and Sepsityper kit from Bruker (Billerica, MA, United States) could create massive synergy in rapid sepsis diagnosis. By eliminating the subculture process and using the PBCB directly in AST, I was able to get the AST result 1 day sooner. Moreover, if the AST method could be performed in six hours, the AST result could be available within 24 hours after blood collection. Combining direct ID using MALDI-TOF MS and DRAST will enable the ID and AST information to be provided on the same day as the detection of the bacteria from the blood.

The blood culture step must be shortened for further time reduction of AST from blood collection as the DRAST system requires only  $10^5$  CFU/ml of bacteria for AST, a value that is 10,000-fold smaller than the current bacterial concentration in positive blood culture bottles. I propose the possibility of usage of ultrasensitive microbial isolation technology for rapid purified microbial culture. If this technology is realized in near future, the whole sepsis diagnosis may be available within a day, from blood extraction to results. If new rapid purified microbial system capable of detecting positivity of microbes at an earlier stage is integrated

with the DRAST system, the total time required for AST from blood collection would be within a day even considering working hours in clinical settings. This integrative approach could change the paradigm of antimicrobial prescription in the clinic and increase the survival rates of sepsis patients.

# Bibliography

1. Bone, R.C., *The Pathogenesis of Sepsis*. Annals of Internal Medicine, 1991. **115**(6): p. 457-469.
2. Fleischmann, C., et al., *Assessment of Global Incidence and Mortality of Hospital-treated Sepsis. Current Estimates and Limitations*. American Journal of Respiratory and Critical Care Medicine, 2016. **193**(3): p. 259-272.
3. Fleischmann-Struzek, C., et al., *The global burden of paediatric and neonatal sepsis: a systematic review*. The Lancet Respiratory Medicine, 2018. **6**(3): p. 223-230.
4. Gaieski, D.F., et al., *Benchmarking the Incidence and Mortality of Severe Sepsis in the United States\**. Critical Care Medicine, 2013. **41**(5): p. 1167-1174.
5. Reimer, L.G., M.L. Wilson, and M.P. Weinstein, *Update on detection of bacteremia and fungemia*. Clinical Microbiology Reviews, 1997. **10**(3): p. 444-465.
6. Bone, R.C., et al., *Definitions for Sepsis and Organ Failure and Guidelines for the Use of Innovative Therapies in Sepsis*. Chest, 1992. **101**(6): p. 1644-1655.
7. Dellinger, R.P., et al., *Surviving Sepsis Campaign: International guidelines for management of severe sepsis and septic shock: 2008*. Intensive Care Medicine, 2008. **34**(1): p. 17-60.
8. Levy, S.B. and B. Marshall, *Antibacterial resistance worldwide: causes, challenges and responses*. Nature Medicine, 2004. **10**(12): p. S122-S129.
9. Angus, D.C., et al., *Epidemiology of severe sepsis in the United States: Analysis of incidence, outcome, and associated costs of care*. Critical Care Medicine, 2001. **29**(7): p. 1303-1310.
10. Patel, M., *Utility of blood culture in sepsis diagnostics*. Journal of The Academy of Clinical Microbiologists, 2016. **18**(2): p. 74-79.
11. Choi, J., et al., *Direct, rapid antimicrobial susceptibility test from positive blood cultures based on microscopic imaging analysis*. Scientific Reports, 2017. **7**(1): p. 1148.
12. Pammi, M., et al., *Molecular Assays in the Diagnosis of Neonatal Sepsis: A Systematic Review and Meta-analysis*. Pediatrics, 2011. **128**(4): p. e973-e985.
13. Reddy, B., et al., *Point-of-care sensors for the management of sepsis*. Nature Biomedical Engineering, 2018. **2**(9): p. 640-648.
14. Seymour, C.W., et al., *Time to Treatment and Mortality during*

- Mandated Emergency Care for Sepsis*. New England Journal of Medicine, 2017. **376**(23): p. 2235–2244.
15. Kralik, P. and M. Ricchi, *A Basic Guide to Real Time PCR in Microbial Diagnostics: Definitions, Parameters, and Everything*. Frontiers in Microbiology, 2017. **8**(108).
  16. Li, Y., X. Yang, and W. Zhao, *Emerging Microtechnologies and Automated Systems for Rapid Bacterial Identification and Antibiotic Susceptibility Testing*. SLAS TECHNOLOGY: Translating Life Sciences Innovation, 2017. **22**(6): p. 585–608.
  17. Peitz, I. and R. van Leeuwen, *Single-cell bacteria growth monitoring by automated DEP-facilitated image analysis*. Lab on a Chip, 2010. **10**(21): p. 2944–2951.
  18. Sinn, I., et al., *Asynchronous magnetic bead rotation (AMBR) biosensor in microfluidic droplets for rapid bacterial growth and susceptibility measurements*. Lab on a Chip, 2011. **11**(15): p. 2604–2611.
  19. Kalashnikov, M., et al., *A microfluidic platform for rapid, stress-induced antibiotic susceptibility testing of Staphylococcus aureus*. Lab on a Chip, 2012. **12**(21): p. 4523–4532.
  20. Price, C.S., S.E. Kon, and S. Metzger, *Rapid antibiotic susceptibility phenotypic characterization of Staphylococcus aureus using automated microscopy of small numbers of cells*. Journal of Microbiological Methods, 2014. **98**: p. 50–58.
  21. Schoepp, N.G., et al., *Digital Quantification of DNA Replication and Chromosome Segregation Enables Determination of Antimicrobial Susceptibility after only 15 Minutes of Antibiotic Exposure*. Angewandte Chemie International Edition, 2016. **55**(33): p. 9557–9561.
  22. Schoepp, N.G., et al., *Rapid pathogen-specific phenotypic antibiotic susceptibility testing using digital LAMP quantification in clinical samples*. Science Translational Medicine, 2017. **9**(410): p. eaal3693.
  23. Choi, J., et al., *Rapid drug susceptibility test of Mycobacterium tuberculosis using microscopic time-lapse imaging in an agarose matrix*. Applied Microbiology and Biotechnology, 2016. **100**(5): p. 2355–2365.
  24. Choi, J., et al., *A rapid antimicrobial susceptibility test based on single-cell morphological analysis*. Science Translational Medicine, 2014. **6**(267): p. 267ra174–267ra174.
  25. Kim, H., et al., *Clinical Evaluation of QMAC-dRAST for Direct and Rapid Antimicrobial Susceptibility Test with Gram-Positive Cocci from Positive Blood Culture Bottles*. Ann Clin Microbiol, 2018. **21**(1): p. 12–19.

26. Song, S.W., et al., *High-Throughput Screening: One-Step Generation of a Drug-Releasing Hydrogel Microarray-On-A-Chip for Large-Scale Sequential Drug Combination Screening (Adv. Sci. 3/2019)*. Advanced Science, 2019. **6**(3): p. 1970014.
27. Svedberg, G., et al., *Towards encoded particles for highly multiplexed colorimetric point of care autoantibody detection*. Lab on a Chip, 2017. **17**(3): p. 549–556.
28. Song, S.W., Y. Jeong, and S. Kwon, *Photocurable Polymer Nanocomposites for Magnetic, Optical, and Biological Applications*. IEEE Journal of Selected Topics in Quantum Electronics, 2015. **21**(4): p. 324–335.
29. Song, Y., et al., *Liquid-capped encoded microcapsules for multiplex assays*. Lab on a Chip, 2017. **17**(3): p. 429–437.
30. Lee, H., et al., *Colour-barcoded magnetic microparticles for multiplexed bioassays*. Nature Materials, 2010. **9**(9): p. 745–749.
31. Han, S., et al., *An encoded viral micropatch for multiplex cell-based assays through localized gene delivery*. Lab on a Chip, 2017. **17**(14): p. 2435–2442.
32. Bae, H.J., et al., *Biomimetic Microfingerprints for Anti-Counterfeiting Strategies*. Advanced Materials, 2015. **27**(12): p. 2083–2089.
33. Choi, J., et al., *Rapid antibiotic susceptibility testing by tracking single cell growth in a microfluidic agarose channel system*. Lab on a Chip, 2013. **13**(2): p. 280–287.
34. Song, S.W., et al., *Uniform Drug Loading into Prefabricated Microparticles by Freeze-Drying*. Particle & Particle Systems Characterization, 2017. **34**(5): p. 1600427.
35. Brook, I., *Inoculum Effect*. Clinical Infectious Diseases, 1989. **11**(3): p. 361–368.
36. Jorgensen, J.H. and M.J. Ferraro, *Antimicrobial susceptibility testing: a review of general principles and contemporary practices*. Clin Infect Dis, 2009. **49**(11): p. 1749–55.
37. Waters, C.M. and B.L. Bassler, *QUORUM SENSING: Cell-to-Cell Communication in Bacteria*. Annual Review of Cell and Developmental Biology, 2005. **21**(1): p. 319–346.
38. Miller, M.B. and B.L. Bassler, *Quorum sensing in bacteria*. Annu Rev Microbiol, 2001. **55**(1): p. 165–99.
39. Soriano, F., et al., *Correlation of pharmacodynamic parameters of five beta-lactam antibiotics with therapeutic efficacies in an animal model*. Antimicrobial agents and chemotherapy, 1996. **40**(12): p. 2686–2690.
40. Soriano, F., R. Edwards, and D. Greenwood, *Effect of inoculum size*

- on bacteriolytic activity of cefminox and four other beta-lactam antibiotics against *Escherichia coli*. Antimicrobial agents and chemotherapy, 1992. **36**(1): p. 223-226.
41. Udekwu, K.I., et al., *Functional relationship between bacterial cell density and the efficacy of antibiotics*. Journal of Antimicrobial Chemotherapy, 2009.
  42. Thomson, K.S. and E.S. Moland, *Cefepime, piperacillin-tazobactam, and the inoculum effect in tests with extended-spectrum beta-lactamase-producing Enterobacteriaceae*. Antimicrobial Agents and Chemotherapy, 2001. **45**(12): p. 3548-3554.
  43. Wikler, M.A., et al., *Methods for dilution antimicrobial susceptibility tests for bacteria that grow aerobically: approved standard*. 2012. **29**.
  44. Faron, M.L., B.W. Buchan, and N.A. Ledebor, *Matrix-Assisted Laser Desorption Ionization-Time of Flight Mass Spectrometry for Use with Positive Blood Cultures: Methodology, Performance, and Optimization*. Journal of Clinical Microbiology, 2017. **55**(12): p. 3328-3338.
  45. Services, U.S.D.o.H.a.H., *Class II Special Controls Guidance Document: Antimicrobial Susceptibility Test (AST) Systems*, F.a.D. Administration, Editor. 2009.
  46. Chen, J.R., et al., *Rapid identification and susceptibility testing using the VITEK (R) 2 system using culture fluids from positive BacT/ALERT (R) blood cultures*. Journal of Microbiology Immunology and Infection, 2008. **41**(3): p. 259-264.
  47. de Cueto, M., et al., *Use of positive blood cultures for direct identification and susceptibility testing with the Vitek 2 system*. Journal of Clinical Microbiology, 2004. **42**(8): p. 3734-3738.
  48. Howard, W.J., et al., *Vitek GPS card susceptibility testing accuracy using direct inoculation from BACTEC 9240 blood culture bottles*. Diagnostic Microbiology and Infectious Disease, 1996. **24**(2): p. 109-112.
  49. Woods, G.L., D. Latemple, and C. Cruz, *EVALUATION OF MICROSCAN RAPID GRAM-POSITIVE PANELS FOR DETECTION OF OXACILLIN-RESISTANT STAPHYLOCOCCI*. Journal of Clinical Microbiology, 1994. **32**(4): p. 1058-1059.
  50. Ligozzi, M., et al., *Evaluation of the VITEK 2 system for identification and antimicrobial susceptibility testing of medically relevant gram-positive cocci*. Journal of Clinical Microbiology, 2002. **40**(5): p. 1681-1686.
  51. *Direct antimicrobial susceptibility testing guidelines*. 2012, The European Committee on Antimicrobial Susceptibility Testing: 4010 Basel SWITZERLAND.

52. Choi, J., et al., *A rapid antimicrobial susceptibility test based on single-cell morphological analysis*. *Sci Transl Med*, 2014. **6**(267): p. 267ra174.
53. Pavlaki, M., et al., *Polymicrobial bloodstream infections: epidemiology and impact on mortality*. *Journal of Global Antimicrobial Resistance*, 2013. **1**(4): p. 207-212.
54. Lin, J.N., et al., *Characteristics and outcomes of polymicrobial bloodstream infections in the emergency department: a matched case-control study*. *Academic Emergency Medicine*, 2010. **17**(10): p. 1072-1079.
55. Buchan, B.W., K.M. Riebe, and N.A. Ledebor, *Comparison of the MALDI Biotyper System Using Sepsityper Specimen Processing to Routine Microbiological Methods for Identification of Bacteria from Positive Blood Culture Bottles*. *Journal of Clinical Microbiology*, 2012. **50**(2): p. 346-352.
56. Mahe, P., et al., *Automatic identification of mixed bacterial species fingerprints in a MALDI-TOF mass-spectrum*. *Bioinformatics*, 2014. **30**(9): p. 1280-1286.
57. Fiori, B., et al., *Performance of two resin-containing blood culture media in the detection of bloodstream infections and in direct MALDI-TOF broth assays for isolate identification: clinical comparison of the BacT/ALERT Plus and BACTEC Plus Systems*. *Journal of clinical microbiology*, 2014: p. JCM. 01171-14.
58. Barenfanger, J., C. Drake, and G. Kacich, *Clinical and financial benefits of rapid bacterial identification and antimicrobial susceptibility testing*. *Journal of Clinical Microbiology*, 1999. **37**(5): p. 1415-1418.
59. Trenholme, G.M., et al., *Clinical Impact of Rapid Identification and Susceptibility Testing of Bacterial Blood Culture Isolates*. *Journal of Clinical Microbiology*, 1989. **27**(6): p. 1342-1345.
60. Doern, G.V., et al., *Clinical Impact of Rapid in-Vitro Susceptibility Testing and Bacterial Identification*. *Journal of Clinical Microbiology*, 1994. **32**(7): p. 1757-1762.
61. Olsen, R.J., P.L. Cernoch, and J.M. Musser, *Integrating rapid pathogen identification and antimicrobial stewardship significantly decreases hospital costs*. *Archives of pathology & laboratory medicine*, 2013. **137**(9): p. 1247.
62. Patel, J.B., et al., *Performance Standards for Antimicrobial Susceptibility Testing; Twenty-Fifth Informational Supplement*. 2015. **35**.
63. Christner, M., et al., *Rapid identification of bacteria from positive blood culture bottles by use of matrix-assisted laser desorption-*

*ionization time of flight mass spectrometry fingerprinting. Journal of clinical microbiology, 2010. 48(5): p. 1584-1591.*

## 국문 초록

패혈증은 미생물 감염으로 인해 전신에 심각한 염증 반응이 나타나는 증세이다. 패혈증 환자의 생존율은 시간당 9%씩 감소하며, 매년 전 세계적으로 1,800만 명의 패혈증 환자가 발생하고 있는 실정이다. 패혈증 환자의 30일 이내의 사망률은 20~30%로 고위험 질병군으로 알려진 뇌졸중, 심근경색보다도 2~3배 이상 높은 수치이다. 이러한 패혈증 환자의 치료를 위해서는 빠른 시간 이내에 환자에게 알맞은 최적 항균제 처방에 필요한 환자의 항균제에 대한 내성 확인이 필수적이다. 기존의 패혈증 진단에는 패혈증 환자로부터 채혈에서 항균제 감수성 검사 종료까지 만 3일이 소요된다. 패혈증 환자의 혈액에는 1~10 CFU/mL 수준의 낮은 수의 병원균이 존재하므로 항균제 감수성 검사 수행을 위해서는 병원균 수의 증가 과정인 혈액 배양 과정이 필수적이다. 혈액 배양 이후에는 혈액과 혼합되어 있는 병원균을 분리하기 위한 분리 배양 과정이 추가적으로 수행된다. 이후 항균제 감수성 검사를 통해 패혈증 환자에게 필요한 최적 항균제를 확인할 수 있다. 본 연구 그룹은 오랜 시간이 소요되는 패혈증 진단을 줄이기 위하여 미생물 고정 기술 및 단일 세포 형태 분석 기술을 제안한 바

있으며, 이를 통해 12시간 소요되는 항균제 감수성 검사 수행 시간을 3시간으로 단축하는 데 성공한 바 있다. 그러나 여전히 패혈증 진단에는 많은 시간이 소요된다는 한계가 존재하였다.

본 논문에서는 현재의 패혈증 진단 과정에서 분리 배양 없이 혈액 배양 이후 바로 항균제 감수성 검사를 수행할 수 있는 기술을 제안하였으며, 이를 성공적으로 개발하였다. 본 논문에서는 미세패턴이 새겨진 96웰 형태의 대용량 고효율 바이오칩을 활용하였으며, 바이오칩 웰 내부의 미세패턴은 샘플의 안정적인 로딩을 가능하게 하였다. 또한 본 논문에서는 본 연구 그룹에서 이전 연구에서 활용한 수평 확산 기법이 아닌 수직 확산 기법을 이용하였다. 수평 확산 기법의 경우 항균제의 확산 거리에 따른 병원균의 반응이 균일하지 않기 때문에 아가로즈 내의 병원균의 대면적 이미징이 필요한 본 기술에 적합하지 않았다. 따라서 본 논문에서는 항균제의 수직 확산을 이용해 병원균과 아가로즈 수화젤 복합체 내부의 균일한 항균제 분산이 가능하였으며, 이를 통해 아가로즈 내부에서의 동일 항균제 종류 및 농도에 대해서 병원균의 균일한 반응을 확인할 수 있었다. 본 논문에서는 실제 미생물 진단 검사실에서 활용 가능한 수준으로 약물 처리를 하고자 노력하였으며, 동결 건조 기법을 활용해 실제 검사를 수행할 때에는 배양액을 일괄적으로 위성 웰에 인가하는 기술적 편리함을 부가하였다.

본 논문의 바이오칩은 각 웰에 포커스 마크 (Focus mark)를 새겨져 있기 때문에 병원균의 항균제 감수성 판단 시에 동일한 위치에서 타임랩스 (Time-lapse)로 자동으로 이미징을 할 수 있었다. 이렇게 타임랩스로 획득한 이미지를 이미징 프로세싱을 통해서 각 농도에 대한 감수성을 확인하고 미생물 동정 결과에 기반하여 저항성/감수성 분석을 수행할 수 있었다.

이러한 분리 배양을 거치지 않고, 혈액 배양 양성 검체를 이용해 고속 항균제 감수성 검사를 통해서 확인한 약물 반응을 말디토프 질량분석기를 통해 얻은 미생물 동정 결과를 기반으로 분석하였으며, 이러한 접근법을 이용하여 임상 현장에서 약 300여개의 병원균 검체를 대상으로 초고속 항균제 감수성 검사를 수행하였다. 본 논문에서 개발한 초고속 항균제 감수성 검사법은 기존의 60시간 이상 소요되는 패혈증 진단 과정을 반 이하로 줄이는데 성공하였으며, 미국 민간 표준 연구소에서 제시하는 표준 정확도 및 불일치도 기준을 만족시켰다.

정리해보면, 본 연구에서 제시한 플랫폼은 다음과 같은 의의를 가진다. 분리 배양 과정 없이도 기존에 3일 소요되는 패혈증 진단 과정을 30시간 이내로 단축시킨 초고속 항균제 감수성 검사 기술로서, 한시라도 최적 항균제 처방이 필요한 패혈증 환자에게 빠른 시간 이내에 최적 항균제 처방을 가능하게 해준다. 또한 실제 임상 현장에서 활용

가능한 자동화에 가까운 수준의 시스템을 개발함으로써 이러한 장점은 의료 현장에서의 초고속 항균제 감수성 검사 기술의 활용성을 높인 것이다. 이런 장점들로 인해 지금껏 고통 받는 패혈증 환자에게 더 빠른 시간 이내에 최적 항균제 처방이 가능해지고, 최근 전세계적으로 문제가 되고 있는 항균제 내성 문제 해결에 기여할 수 있을 것으로 기대한다.

**주요어** : 패혈증, 초고속 항균제 감수성 검사, 바이오칩, 단일 군집 추적, 항균제 내성

**학번** : 2014-24882